

A STUDY OF GAS SOLUBILITIES AND TRANSPORT  
PROPERTIES IN FUEL CELL ELECTROLYTES

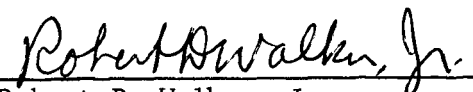
Research Grant NGR 10-005-022

Fifth Semi-Annual Report

Period Covered: September 1, 1967 - February 29, 1968

Prepared For  
National Aeronautics and Space Administration  
Washington, D. C.

May 24, 1968

  
Robert D. Walker, Jr.  
Principal Investigator

ENGINEERING AND INDUSTRIAL EXPERIMENT STATION  
College of Engineering  
University of Florida  
Gainesville, Florida

## TABLE OF CONTENTS

	<u>Page</u>
LIST OF TABLES.....	ii
LIST OF FIGURES.....	iii
1.0 SUMMARY.....	1
2.0 SOLUBILITY OF GASES IN POTASSIUM HYDROXIDE SOLUTIONS...	2
2.1 Theories of Gas Solubility.....	2
2.2 Experimental Procedures.....	11
2.3 Experimental Results.....	12
2.4 Test of Scaled Particle Theory.....	22
3.0 DIFFUSION COEFFICIENTS OF OXYGEN AND HYDROGEN IN POTASSIUM HYDROXIDE SOLUTION.....	41
3.1 Experimental.....	41
3.1.1 Presaturation of Gases.....	41
3.1.2 Procedure.....	41
3.1.3 Pretreatment of Electrodes.....	42
3.2 Result and Discussion.....	43
4.0 VAPOR PRESSURES OF LITHIUM HYDROXIDE SOLUTIONS.....	51
4.1 Apparatus.....	51
4.2 Experimental Procedure.....	53
4.3 Experimental Results.....	55
5.0 SOLUBILITIES OF GASES IN LITHIUM HYDROXIDE SOLUTIONS...	59
5.1 Experimental.....	59
5.2 Results.....	59
6.0 FUTURE PLANS.....	62
REFERENCES.....	63

# LIST OF TABLES

<u>Table</u>		<u>Page</u>
2.3-1	Solubility of Various Gases in Water, (g.mole/ liter) $\times 10^3$ .....	13
2.3-2	Activity Coefficients of Solute Gases in KOH Solutions.....	16
2.4-1	Properties and Parameters for Solvent Species.....	26
2.4-2	Properties and Parameters for the Solutes.....	26
2.4-3	Comparison of Theoretical and Experimental Values of $\ln(\gamma_{\alpha} K_{\alpha})$ .....	31
2.4-4	$\Delta \bar{H}_2$ for $O_2/20\%$ KOH Solution, cal.(g.mole) $^{-1}$ .....	38
2.4-5	Parameter for $\sigma$ for Solvent Species, $A^0$ .....	38
3.2-1	Diffusion Coefficients of Oxygen in KOH Solution..	45
3.2-2	Diffusion Coefficients of Hydrogen in KOH Solution	45
4.2-1	Vapor Pressures of Lithium Hydroxide Solutions....	56
5.2-1	Solubility of Gases in Aqueous Lithium Hydroxide Solutions.....	60

# LIST OF FIGURES

<u>Figure</u>		<u>Page</u>
2.3-1	Activity Coefficients of Hydrogen at 25°C.....	19
2.3-2	Activity Coefficients of Oxygen at 25°C.....	20
2.4-1	Experimental $\ln(\gamma_{\alpha} K_{\alpha})$ vs. Polarizability for Solubility of Rare Gases in Water at 25°C.....	23
2.4-2	Theoretical and Experimental Activity Coefficients of Oxygen at 25°C.....	34
2.4-3	Effect of Temperature on Activity Coefficient of Oxygen in 20% KOH Solution.....	36
3.2-1	Diffusion Coefficients of O <sub>2</sub> in KOH Solutions.....	46
3.2-2	Diffusion Coefficients of H <sub>2</sub> in KOH Solutions.....	47
3.2-3	Diffusion Coefficients of O <sub>2</sub> vs Species Fraction of KOH.....	48
3.2-4	Diffusion Coefficients of H <sub>2</sub> vs Species Fraction of KOH.....	49
3.2-5	Plot of $\ln(\frac{D}{T})$ vs $\frac{1}{T}$ .....	50
4.1-1	Glass Vapor Pressure Apparatus.....	52
4.1-2	Stainless Steel Vapor Pressure Apparatus for High Pressure Measurement.....	54
4.2-1	Vapor Pressure of LiOH vs Concentration.....	57
4.3-1	Vapor Pressure vs $\frac{1}{T}$ for LiOH Solutions.....	58
5.2-1	Solubility of Oxygen and Argon in LiOH Solutions..	61

## 1.0 SUMMARY

During this report period major efforts were directed to (1) development of a theoretical treatment of solubility, (2) measurements of the vapor pressure of LiOH solutions, (3) measurements of gas solubilities in LiOH solutions, and (4) measurements of gas diffusivities in KOH solutions.

The "cavity" model has been extended to cover the solubility of gases in concentrated solutions of electrolytes and the predictions of the theory have been compared with the experimental results for a number of non-polar gases dissolved in KOH over a wide range of concentrations and temperatures. Agreement between theory and experiment is good for small solute molecules; the results for sulfur hexafluoride and neo-pentane disagree with theory by substantial amounts, but the agreement is much better than for other theories.

Vapor pressures over LiOH solutions have been measured at temperatures up to 60°C and at concentrations of LiOH to just over 10 wt. % by means of a dew point method. Agreement of these data with the few which are in the literature is very good.

The solubility of oxygen and argon in aqueous LiOH solutions has been measured over the temperature range 25-60°C and at LiOH concentrations up to near saturation. The solubility of these two gases decreases substantially as either LiOH concentration or temperature increases.

Measurements of the diffusivity of oxygen in KOH solution from 25 to 60°C and of hydrogen at 25 and 40°C have been made in KOH

concentrations up to saturation using an electrochemical method based on diffusion in a capillary. A semi-log plot of  $D$  vs species fraction is approximately linear up to moderate KOH concentrations, but it becomes curved towards flatness at high KOH concentrations, i.e., the diffusivity tends to approach a constant value at high KOH concentrations. A log-log plot of  $D/T$  vs  $1/T$  is linear for all KOH concentrations, over the temperature range so far studied.

## 2.0 SOLUBILITY OF GASES IN POTASSIUM HYDROXIDE SOLUTIONS - S. K. Shoor

In continuation of work reported previously, measurements of the solubility of oxygen, hydrogen, helium, argon, sulfur hexafluoride, methane and neopentane have been made at temperatures of 25, 40, 60, 80°C. Solubilities of oxygen and hydrogen have also been measured at 100°C. These data have been utilized in the evaluation of a theoretical model for solubilities of gases in concentrated electrolytic solutions.

### 2.1 Theories of Gas Solubility

Theories of gas solubility in nonelectrolytic liquids have been reviewed by Battino and Clever (1). Recently, Conway (2) has summarized the important modifications of the electrostatic theories for electrolytic systems. All of the electrostatic theories assume the solvent to be a continuous medium and apply only to dilute electrolyte solutions.

A cavity model based on scaled particle theory (3,4) has been developed, and it can be used to predict gas solubilities in concentrated potassium hydroxide solutions with moderately good

accuracy. We consider a mixture consisting of components 1,2, ----, m (the solvent). Into this mixture a solute molecule  $\alpha$  is introduced. The real molecules are assumed to possess hard cores of diameter  $a_1, \dots, a_m, a_\alpha$ . Assuming that the total potential energy is the sum of pair potentials, the following expression for chemical potential of the solute can be obtained (5).

$$\mu_\alpha = kT \ln \rho_\alpha \Lambda_\alpha^3 + \sum_{j=1}^m \rho_j \int_0^\infty dr \int_\xi \frac{\partial u_{\alpha j}(r, \xi)}{\partial \xi} g_{\alpha j}(r, \xi) 4\pi r^2 d\xi \quad (2.1-1)$$

where  $\Lambda = \left( \frac{h^2}{2\pi m k T} \right)$

$\rho_j$  = number density of component j

$u_{\alpha j}(r, \xi)$  = pair wise potential between solute and solvent component j

$g_{\alpha j}(r, \xi)$  = radial distribution function between solute and solvent component j

$\xi$  = a charging parameter (see ref. 14) which allows the solute molecule to be coupled with the solvent.

We note that only interactions between the solute  $\alpha$  and solvent of species j are involved in this equation. In Equation 2.1-1 the lower and upper integration limits of  $\xi$  correspond to complete uncoupling and complete coupling of the solute molecule, respectively.

The pair potential  $u_{\alpha j}(r, \xi)$  is assumed to be of the following form

$$u_{\alpha j}(r, \xi) = u_{\alpha j}^h(r, \xi_h) + u_{\alpha j}^s(r, \xi_s) \quad (2.1-2)$$

where  $u_{\alpha j}^h(r, \xi_h)$  and  $u_{\alpha j}^s(r, \xi_s)$  are the hard sphere and soft portions of the potential between solute and solvent component j, respectively, and  $\xi_h$  and  $\xi_s$  are charging parameters for the hard and soft potentials, respectively.

$$u_{\alpha j}^h(r) = \infty \quad r \leq a_{\alpha j} = \frac{a_\alpha + a_j}{2} \quad (2.1-3)$$

$$\left. \begin{aligned} u_{\alpha j}^h(r) &= 0 \\ u_{\alpha j}^s(r, \xi_s) &= \xi_s u_{\alpha j}^s(r) \end{aligned} \right\} \quad r > a_{\alpha j}$$

By allowing  $\xi_h$  to vary from 0 to  $a_{\alpha j}$  we "charge up" the hard part of the potential. The term  $\xi_h$  is the 'scaling' parameter (hence the name 'scaled particle theory'); thus, when  $\xi_h = a_{\alpha j}$  the hard core of solute  $\alpha$  is fully coupled to the rest of the system.  $\xi_s$  varies from 0 to 1. When  $\xi_s = 1$ , the soft part of the potential will be fully coupled. A value of zero assigned to both  $\xi_h$  and  $\xi_s$  implies that solute  $\alpha$  is decoupled from the system.

The solute chemical potential may now be written

$$\mu_\alpha = kT \ln \rho_\alpha \Lambda_\alpha^3 + \bar{g}_\alpha^h + \bar{g}_\alpha^s \quad (2.1-4)$$

where

$$\bar{g}_\alpha^h = \sum_{j=1}^m \rho_j \int_{\xi_h=0}^{\xi_h=a_{\alpha j}} d\xi_h \int_{r=0}^{\infty} \frac{\partial u_{\alpha j}^h(r, \xi_h)}{\partial \xi_h} g_{\alpha j}(r, \xi_h, \xi_s=0) 4\pi r^2 dr \quad (2.1-5)$$

$$\bar{g}_\alpha^s = \sum_{j=1}^m \rho_j \int_{\xi_s=0}^{\xi_s=1} d\xi_s \int_{a_{\alpha j}}^{\infty} u_{\alpha j}(r) g_{\alpha j}(r, \xi_h=a_{\alpha j}, \xi_s) 4\pi r^2 dr \quad (2.1-6)$$

The charging procedure involved in Equation 2.1-5 is tantamount to first introducing a hard-sphere solute molecule of diameter  $a_\alpha$ . In evaluating  $\bar{g}_\alpha^h$  a solute molecule of diameter  $(-a_\alpha)$  is introduced, and then scaled up to its full diameter  $a_\alpha$ .



For a vapor and liquid phase in equilibrium

$$\mu_{\alpha}^G = \mu_{\alpha}^L \quad (2.1-7)$$

where  $\mu_{\alpha}^G$  and  $\mu_{\alpha}^L$  are the chemical potentials of the solute molecule in the gas and liquid phases, respectively. The chemical potential,  $\mu_{\alpha}^G$ , can be written (5) as

$$\mu_{\alpha}^G = kT \ln \left( \frac{\Lambda_{\alpha}^3}{kT} \right) + kT \ln f_{\alpha}^G \quad (2.1-8)$$

where  $f_{\alpha}^G$  is the fugacity of the solute molecule in the gas phase.

By equating Equations 2.1-4 and 2.1-8 one obtains

$$\ln \left( \frac{f_{\alpha}^G}{\rho_{\alpha}} \right) = \frac{-\bar{h}_{\alpha}}{kT} + \frac{-\bar{s}_{\alpha}}{kT} + \ln kT \quad (2.1-9)$$

The mole fraction is given by

$$x_{\alpha} = \frac{\rho_{\alpha}}{\sum_j \rho_j}$$

where  $\rho_i$  is the number of molecules of species i per unit volume

$$\ln \left( \frac{f_{\alpha}^G}{x_{\alpha}} \right) = \frac{-\bar{h}_{\alpha}}{kT} + \frac{-\bar{s}_{\alpha}}{kT} + \ln(kT \sum_j \rho_j) \quad (2.1-10)$$

or, in terms of partial molal quantities,

$$\ln \left( \frac{f_{\alpha}^G}{x_{\alpha}} \right) = \frac{-\bar{G}_{\alpha}^h}{RT} + \frac{-\bar{G}_{\alpha}^s}{RT} + \ln \left( \frac{RT}{V} \sum_j n_j \right) \quad (2.1-11)$$

where  $\sum_j n_j$  = number of moles in volume V.

From classical thermodynamics, we have

$$\frac{f_{\alpha}}{x_{\alpha}} = \gamma_{\alpha} K_{\alpha}$$

where  $\gamma_\alpha$  is the activity coefficient of solute  $\alpha$  in the solution and  $K$  is the Henry's law constant defined as

$$\lim_{x_\alpha \rightarrow 0} f_\alpha = K_\alpha x_\alpha$$

$$x_\alpha \rightarrow 0$$

$$x_j = 0$$

$$j \neq \alpha$$

Thus, Equation 2.1-10 can now be written as

$$\ln(\gamma_\alpha K_\alpha) = \frac{\bar{g}_\alpha^h}{kT} + \frac{\bar{g}_\alpha^s}{kT} + \ln\left(\frac{RT}{V} \sum_j n_j\right) \quad (2.1-12)$$

Evaluation of  $\bar{g}_\alpha^h$ :

From Equation 2.1-5 we have

$$\bar{g}_\alpha^h = \sum_{j=1}^m \rho_j \int_{\xi_h=0}^{\xi_h=a_{\alpha j}} d\xi_h \int_{r=0}^{\infty} \frac{\partial u_{\alpha j}^h(r, \xi_h)}{\partial \xi_h} g(r, \xi_h, \xi_s=0) 4\pi r^2 dr$$

By applying the treatment of Reiss et al. (3) to a mixture containing  $m$  solvent components and assuming that the concentration of solute is very low so that  $u = 0$ , it can be shown that

$$\bar{g}_\alpha^h = \sum_{j \neq \alpha} \rho_j \int_0^{\xi_h=a_{\alpha j}} G_{\alpha j}(r) 4\pi r^2 dr \quad (2.1-13)$$

where  $G_{\alpha j}(r)$  is the radial distribution function for solvent component  $j$  around a solute molecule  $\alpha$  when the two are in contact. The quantity on the right hand side of Equation 2.1-13 can be shown to be equal to the work of introducing a cavity of radius  $\frac{a_\alpha}{2}$  into the solvent, which we term  $W(a_\alpha/2)$ .

Reiss et al. (4) have obtained an expression for  $W(a_\alpha/2)$  from probability considerations based on the relation between the probability of a configuration and the work of creating that configuration (5). Thus

$$W(a_\alpha/2) = -kT \ln \left[ 1 - \frac{4}{3} \pi \sum_{j=1}^m \left( \frac{a_\alpha + a_j}{2} \right)^3 \rho_j \right] \quad \text{for } a_\alpha/2 \leq 0 \quad (2.1-14)$$

From thermodynamic considerations, for very large  $r$ , the following expression for the work of formation of a cavity of radius  $r$  can be written (2,3)

$$W(r) = \frac{4}{3} \pi r^3 p + 4\pi r^2 \sigma_0 \left[ 1 - \frac{2\delta}{r} \right] + f(\rho_j, T) \quad (2.1-15)$$

where  $p$  is the pressure,  $\sigma_0$  is the interfacial tension between the fluid and a perfect rigid wall, and  $\delta$  is a distance of the order of the thickness of the inhomogeneous layer near the interface and accounts for the curvature dependence of the surface work.  $f(\rho_j, T)$  is an arbitrary function of density and temperature, not dependent on  $r$ .

For  $r$  positive but small,  $W(r)$  may be expanded in a Taylor series about  $r=0$  to give

$$W(r) = W(0) + rW'(0) + \frac{1}{2} r^2 W''(0) + K_3 r^3 \quad r > 0 \quad (2.1-16)$$

Since  $W(r)$  and its first two derivatives have been shown (2) to be continuous at  $r = 0$ , the first three coefficients of the series can be evaluated by comparison with Equation 2.1-14. The coefficient of the term in  $r^3$  can be obtained by comparison with Equation 2.1-15,

Thus

$$\frac{W\left(\frac{a_\alpha}{2}\right)}{kT} = -\ln(1-\xi_3) + \left[ \frac{6\xi_2}{1-\xi_3} \right] \frac{a_\alpha}{2} + \left[ \frac{12\xi_1}{1-\xi_3} + \frac{18\xi_2^2}{(1-\xi_3)^2} \right] \left( \frac{a_\alpha}{2} \right)^2 + \frac{4}{3} \pi \frac{p}{kT} \left( \frac{a_\alpha}{2} \right)^3 \quad (2.1-17)$$

where

$$\xi_1 = \frac{1}{6} \pi \sum_{j=1}^m \rho_j (a_j)^1$$

Evaluation of  $\bar{g}_\alpha^s$ :

From Equation 2.1-6 we have

$$\bar{g}_\alpha^s = \sum_{j \neq \alpha}^m \rho_j \int_{\xi_s=0}^{\xi_s=1} d\xi_s \int_{a_{\alpha j}}^{\infty} u_{\alpha j}^s(r) g_{\alpha j}(r, \xi_h = a_{\alpha j}, \xi_s) 4\pi r^2 dr$$

$\bar{g}_\alpha^s$  can be decomposed as follows:

$$\bar{g}_\alpha^s = \bar{e}_\alpha^s - T\bar{s}_\alpha^s + p\bar{v}_\alpha^s \quad (2.1-18)$$

where  $\bar{e}_\alpha^s$ ,  $\bar{v}_\alpha^s$  and  $\bar{s}_\alpha^s$  are, respectively, internal energy, volume and entropy associated with the charging of the soft potential.

At atmospheric pressure the term in  $p\bar{v}_\alpha^s$  can be shown to be small and can be neglected in comparison to  $\bar{e}_\alpha^s$  (6,7). The entropy of charging  $\bar{s}_\alpha^s$  is negative because the system becomes more organized upon charging. Since it is difficult to make a quantitative estimate of this quantity, it will be neglected as a first approximation. The quantity  $\bar{e}_\alpha^s$  can be obtained as follows: Consider a shell of thickness  $dr$  at a distance  $r$  from the solute molecule. The number of particles of solvent component  $j$  in this shell is given by

$$(4\pi r^2 dr) \rho_j g_{\alpha j}(r)$$

If we neglect the volume and entropy terms we have

$$\bar{g}_{\alpha}^s \approx \bar{e}_{\alpha}^s = \sum_{j \neq \alpha}^m \int_{a_{\alpha j}}^{\infty} u_{\alpha j} 4\pi r^2 \rho_j g_{\alpha j}(r) dr \quad (2.1-19)$$

Evaluation of  $\bar{g}_{\alpha}^s$  by the above equation requires a knowledge of  $g_{\alpha j}(r)$ , which is difficult to obtain for the systems studied here. As a first approximation it will be assumed that solvent particles are uniformly distributed around the solute molecule for  $r$  larger than  $a_{\alpha j}$ , i.e.,

$$g_{\alpha j}(r) = 1 \quad r > a_{\alpha j}$$

Thus,

$$\bar{g}_{\alpha}^s \approx \sum_{j \neq \alpha}^m \rho_j \int_{a_{\alpha j}}^{\infty} u_{\alpha j} 4\pi r^2 dr \quad (2.1-20)$$

### Interaction Energy

The interaction energy of the nonpolar solute molecule in an aqueous potassium hydroxide solution consists of nonpolar and electrostatic interactions. It is assumed that for the systems studied here the nonpolar interactions are adequately represented by Lennard-Jones 6-12 potential.

$$\mu_{\alpha j}^{np} = 4\epsilon_{\alpha j} \left[ \left( \frac{\sigma_{\alpha j}}{r} \right)^{12} - \left( \frac{\sigma_{\alpha j}}{r} \right)^6 \right] \quad (2.1-21)$$

The following relations are assumed between pure component Lennard-Jones parameters and those in a mixture:

$$\epsilon_{\alpha j} = (\epsilon_{\alpha} \epsilon_j)^{\frac{1}{2}} \quad \sigma_{\alpha j} = \frac{\sigma_{\alpha} + \alpha_j}{2} \quad (2.1-22)$$

The only electrostatic interaction which must be considered is the induced interaction between a nonpolar solute molecule and the permanent dipole of a water molecule. This interaction, after statistical averaging over all possible orientations, is

$$\mu_{\alpha 1}^{(\mu, \text{ind} \mu)} = - \frac{\mu_1^2 p_{\alpha}}{r^6} \quad (2.1-23)$$

where  $\mu_1$  is the permanent dipole moment of water molecule, and  $p_{\alpha}$  is the polarizability of the solute molecule. It may be noted that, since ions have been assumed to be uniformly distributed around the neutral solute molecule, there is a spherically symmetrical charge distribution around the former molecule. The field intensity due to such a charge distribution at any point in the neutral molecule is zero. For this reason there is no contribution due to the ion-induced dipole interaction.

Thus, the potential energy of interaction of the solute molecule is

$$\Sigma u_{\alpha j} = \sum_{j=1}^3 4\epsilon_{\alpha j} \left[ \left( \frac{\sigma_{\alpha j}}{r} \right)^6 - \left( \frac{\sigma_{\alpha j}}{r} \right)^{12} \right] - \frac{p_{\alpha} \mu_1^2}{r^6} \quad (2.1-24)$$

Substituting Equation 2.1-24 into Equation 2.1-20 gives

$$\begin{aligned} \bar{e}_{\alpha}^s &= - 16\pi \int_{a_{\alpha j}}^{\infty} \sum_{j=1}^3 \rho_j \epsilon_{\alpha j} \left[ \frac{\sigma_{\alpha j}^6}{r^4} - \frac{\sigma_{\alpha j}^{12}}{r^{10}} \right] dr - 4\pi \rho_1 \int_{a_{\alpha j}}^{\infty} \frac{p_{\alpha} \mu_1^2}{r^4} dr \\ &= - 16\pi \left[ \sum_{j=1}^3 \rho_j \epsilon_{\alpha j} \left( \frac{\sigma_{\alpha j}^6}{3a_{\alpha j}^3} - \frac{\sigma_{\alpha j}^{12}}{9a_{\alpha j}^9} \right) \right] - \frac{4\pi \rho_1 p_{\alpha} \mu_1^2}{3a_{\alpha 1}^3} \end{aligned} \quad (2.1-25)$$

At  $a_{\alpha j} = \sigma_{\alpha j}$ ,  $\bar{e}_{\alpha}^s$  can be written as:

$$\bar{e}_{\alpha}^s = - \frac{32\pi}{9} \sum_{j=1}^3 \rho_j \sigma_{\alpha j}^3 \epsilon_{\alpha j} - \frac{4\pi\rho_1 p_{\alpha} \mu_1^2}{3\sigma_{\alpha 1}^3} \quad (2.1-26)$$

## 2.2 Experimental Procedures

The experimental method used for the gas solubility measurements has been previously described in detail by Gubbins, Carden and Walker (10). It involved removal of dissolved gas from a 20 ml sample of the saturated solution by stripping with carrier gas, followed by gas chromatographic analysis.

In determining the solubilities of sulfur hexafluoride and neopentane in solutions containing 31.6 wt % or more potassium hydroxide the amount of dissolved gas was found to be too small to obtain accurate results by the above method. For these systems the following modified procedure was used. The stripped gas, after passing through drying columns, was directed to a concentrator (a tube immersed in a liquid nitrogen bath) where it was condensed from the carrier gas. The gas stream from the concentrator was brought back to chromatograph temperature by passing through a stainless-steel coil immersed in a water bath and it was then returned to the chromatograph.

The following procedure was used to make a measurement: A sample of the KOH solution, saturated with the solute gas, was withdrawn in a syringe and injected into the stripping cell, the concentrator having been previously cooled to liquid nitrogen temperature. At the end of the stripping process (usually 5-10 minutes) the liquid nitrogen bath was removed, whereupon the condensed solute gas evaporated rapidly and passed through the chromatograph to give a sharp peak.

### 2.3 Experimental Results

Each experimental value is the mean of four or more replicate measurements. The precision of the data reported here ranged from approximately 1% at the lowest KOH concentrations (solute mole fractions in the region of  $10^{-5}$ ) to about 5% for the most concentrated KOH solutions ( $10^{-7}$  to  $10^{-8}$  mole fraction solute). The experimental solubility values in water in Table 2.3-1 are compared with values from the literature; in most cases agreement between experimental and literature values is better than 2%.

No previous studies of the solubility in potassium hydroxide solutions of helium, argon, sulfur, hexafluoride, methane and neopentane seem to have been reported. However, several studies have been made of the solubility of oxygen and hydrogen. Geffcken (11) measured solubilities of oxygen and hydrogen at 15° and 25°C in solutions 0 to 1.4M in KOH, and Knaster and Apel'baum (12) made similar measurements at 21°, 45° and 75°C for KOH concentrations up to 10 M. Ruetschi and Amlie (13) have measured solubilities of hydrogen for KOH concentrations up to 10M at 30°C, while Davis et al. (14) recently reported oxygen solubilities at 0°, 25° and 60° for KOH concentrations to 12 M.

To facilitate the comparison of the results of the present investigation with those of previous workers and with theoretical relationships, the data for oxygen and hydrogen at 25°C have been converted to an activity coefficient basis and plotted in Figures 2.3-1 and 2.3-2 in the form of a semi-logarithmic plot. This type of plot has been used since most electrostatic theories of salting-out predict a linear relationship between the logarithm of activity coefficient and the molar



TABLE 2.3-1  
SOLUBILITY OF VARIOUS GASES IN WATER  
(g.mole/liter)  $\times 10^3$

Solute Gas	25°C			40°C			Ref.
	Expt.	Lit.	% Diff.	Expt.	Lit.	% Diff.	
O <sub>2</sub>	1.246	1.263	-1.34	1.049	1.030	+1.84	15
H <sub>2</sub>	0.792	0.784	+1.01	0.713	0.733	-2.73	15
He	0.372	0.378	-1.59	0.371	0.372	-0.27	16,17
Ar	1.400	1.374	+1.89	1.102	1.071	+2.89	16,17
SF <sub>6</sub>	0.223	0.225	-0.89	0.151	-	-	18
CH <sub>4</sub>	1.375	1.341	+2.6	1.046	1.056	-0.95	15
neoC <sub>5</sub> H <sub>12</sub>	0.561	-	-	0.378	-	-	-

Solute Gas	60°C			80°C			Ref.
	Expt.	Lit.	% Diff.	Expt.	Lit.	% Diff.	
O <sub>2</sub>	0.875	0.869	+0.69	0.775	0.786	-1.4	15
H <sub>2</sub>	0.712	0.714	-0.28	-	0.714	-	15
He	0.391	0.392	-0.25	0.430	-	-	16,17
Ar	0.919	0.913	-	0.820	-	-	16,17
SF <sub>6</sub>	0.120	-	-	0.103	-	-	18
CH <sub>4</sub>	0.884	0.872	+1.37	0.779	0.789	-1.27	15
neoC <sub>5</sub> H <sub>12</sub>	0.264	-	-	0.234	-	-	-

Literature value (Ref. 15) of solubility of O<sub>2</sub> in water at 100°C =  $0.758 \times 10^{-3}$  g.mole/liter

Literature value (Ref. 15) of solubility of H<sub>2</sub> in water at 100°C =  $0.714 \times 10^{-3}$  g.mole/liter

concentration of electrolyte, at least for moderate electrolyte concentrations. The equations for calculating activity coefficients are given in the following paragraphs.

Consider a nonideal liquid solution in contact with a vapor phase. For any component  $i$  we can write

$$f_i^G = f_i^L \quad (2.3-1)$$

where superscripts G and L refer to the gas and liquid phases and  $f_i$  is the fugacity of species  $i$ . Subscripts 1, 2 and 3 denote water, solute gas, and potassium hydroxide, respectively. In this work the pressures are sufficiently low so that we can write

$$f_2^G = Py_2 \quad (2.3-2)$$

where  $P$  is the total pressure and  $y_2$  is the mole fraction of solute gas in the gas phase. To get the fugacity in the liquid phase we must first specify a standard state and we choose for this a hypothetical liquid state in which the solute is at infinite dilution in the solvent, i.e.,

$$\lim_{x_2 \rightarrow 0} f_2^O = K_2^O x_2^O \quad (2.3-3)$$

$$x_2 \rightarrow 0$$

$$x_3 = 0$$

where  $K_2^O$  is Henry's Law constant for the gas in pure water,  $f_2^O$  is the fugacity of the dissolved gas, and  $x_2^O$  is the liquid phase mole fraction in the water. The fugacity of the gas dissolved in the electrolyte solution, using this standard state, is

$$f_2^L = K_2^O \gamma_2 x_2 \quad (2.3-4)$$

where  $\gamma_2$  and  $x_2$  are the activity coefficient and the mole fraction in the electrolyte solution. For the systems studied here the values of  $x_2$  are low enough so that Henry's Law should be a good approximation. The term ( $K_2^0 \gamma_2$ ) in Equation 2.3-4 should then be a constant, dependent only on temperature and electrolyte concentration. Combining Equations 2.3-2 and 2.3-4 results in

$$P_{y_2} = K_2^0 \gamma_2 x_2 \quad (2.3-5)$$

Since the pressure involved is about one atmosphere, the gas phase fugacity can be replaced by partial pressure.

Solubilities were determined at a total pressure of one atmosphere, i.e.,  $p_1 = P - p_1^*$ , where  $p_1^*$  is the vapor pressure of water in equilibrium with the electrolyte solution, and these were recalculated to a basis of 1 atm of solute gas by assuming Henry's Law to be applicable. An equation similar to 2.3-5 can be written for water and the two can be combined to give

$$\gamma_2 = \frac{x_2^0(1)}{x_2(1)} \quad (2.3-6)$$

where  $x_2^0(1)$  and  $x_2(1)$  refer to the mole fraction of solute gas in water and KOH solution respectively when the solute partial pressure is 1 atmosphere. In deriving this equation we note that  $\gamma_2^0$  is unity because Henry's Law is assumed to apply.

Activity coefficients calculated from Equation 2.3-6 are presented in Table 2.3-2

TABLE 2.3-2  
ACTIVITY COEFFICIENTS OF SOLUTE GASES IN KOH SOLUTIONS

$$\gamma_2 = x_2^0/x_2$$

KOH Concentration		Activity Coefficient of Oxygen				
Wt. % KOH	<u>g.mole</u> <u>liter</u>	25°C	40°C	60°C	80°C	100°C
0.00	0.00	1.000	1.000	1.000	1.000	1.000
5.00	0.92	1.531	1.535	1.445	1.345	-
13.50	2.67	3.060	2.870	2.580	2.500	-
23.00	5.0	8.150	7.240	6.300	5.730	-
31.61	7.35	20.06	17.80	15.60	14.35	-
40.70	10.12	70.06	53.25	45.30	40.12	10.12
50.30	13.60	-	186.20	-	-	-
50.65	13.75	229.5	-	162.0	142.8	13.75
56.50	16.20	-	-	-	-	16.2

KOH Concentration		Activity Coefficient of Hydrogen				
Wt. % KOH	<u>g.mole</u> <u>liter</u>	25°C	40°C	60°C	80°C	100°C
0.00	0.00	1.000	1.000	1.000	1.000	1.000
5.00	0.92	1.361	1.275	1.319	1.325	-
9.00	1.70	1.710	1.640	1.735	1.810	-
19.50	4.12	3.500	3.290	3.580	3.647	-
32.40	7.6	-	8.700	9.16	9.040	-
34.50	8.17	10.11	-	-	-	-
38.00	9.27	-	-	-	-	15.25
41.40	10.37	20.06	20.40	21.38	21.83	21.87
52.40	14.35	72.00	73.70	76.7	75.4	82.6
56.50	16.20	-	-	-	-	107.5

TABLE 2.3-2 (Continued)

KOH Concentration		Activity Coefficient of Helium			
Wt. % KOH	<u>g.mole</u> liter	25°C	40°C	60°C	80°C
0.00	0.00	1.000	1.000	1.000	1.000
5.00	0.92	1.385	1.360	1.385	1.440
9.00	1.70	1.745	1.725	1.955	1.885
19.00	3.99	3.570	3.710	3.590	3.770
32.40	7.60	13.10	12.65	12.95	13.70

KOH Concentration		Activity Coefficient of Sulfur Hexafluoride			
Wt. % KOH	<u>g.mole</u> liter	25°C	40°C	60°C	80°C
0.00	0.00	1.000	1.000	1.000	1.000
5.00	0.92	2.150	1.968	1.880	1.730
13.50	2.67	7.441	6.530	5.881	4.910
23.00	5.00	43.20	31.90	26.60	22.61
31.6	7.35	234.0	145.5	112.0	84.20

KOH Concentration		Activity Coefficient of Argon			
Wt. % KOH	<u>g.mole</u> liter	25°C	40°C	60°C	80°C
0.00	0.00	1.000	1.000	1.000	1.000
5.00	0.92	1.557	1.480	1.395	1.320
13.50	2.67	3.180	2.810	2.590	2.481
23.0	5.00	7.681	6.925	5.851	5.570
31.61	-	-	-	14.480	13.370
32.40	7.60	22.80	-	-	-
36.60	-	-	31.60	-	-
40.70	-	-	-	-	30.02
41.40	10.37	70.31	58.20	46.10	-

TABLE 2.3-2 (Continued)

KOH Concentration		Activity Coefficient of Methane			
Wt. % KOH	<u>g.mole</u> liter	25°C	40°C	60°C	80°C
0.00	1.000	1.000	1.000	1.000	1.000
5.61	1.03	1.658	1.505	1.480	1.392
13.90	2.77	3.640	3.140	2.831	2.500
23.50	5.13	10.21	8.081	6.901	6.220
31.61	7.35	26.70	19.80	16.65	14.38
40.70	10.12	100.00	63.40	49.60	38.02

KOH Concentration		Activity Coefficient of Neo-Pentane			
Wt. % KOH	<u>g.mole</u> liter	25°C	40°C	60°C	80°C
0.00	0.00	1.000	1.000	1.000	1.000
5.61	1.03	2.180	2.170	2.64	1.935
13.90	2.77	8.910	7.871	6.80	5.940
23.50	5.13	56.10	42.00	33.00	28.60
31.61	7.35	288.0	219.5	158.0	137.5

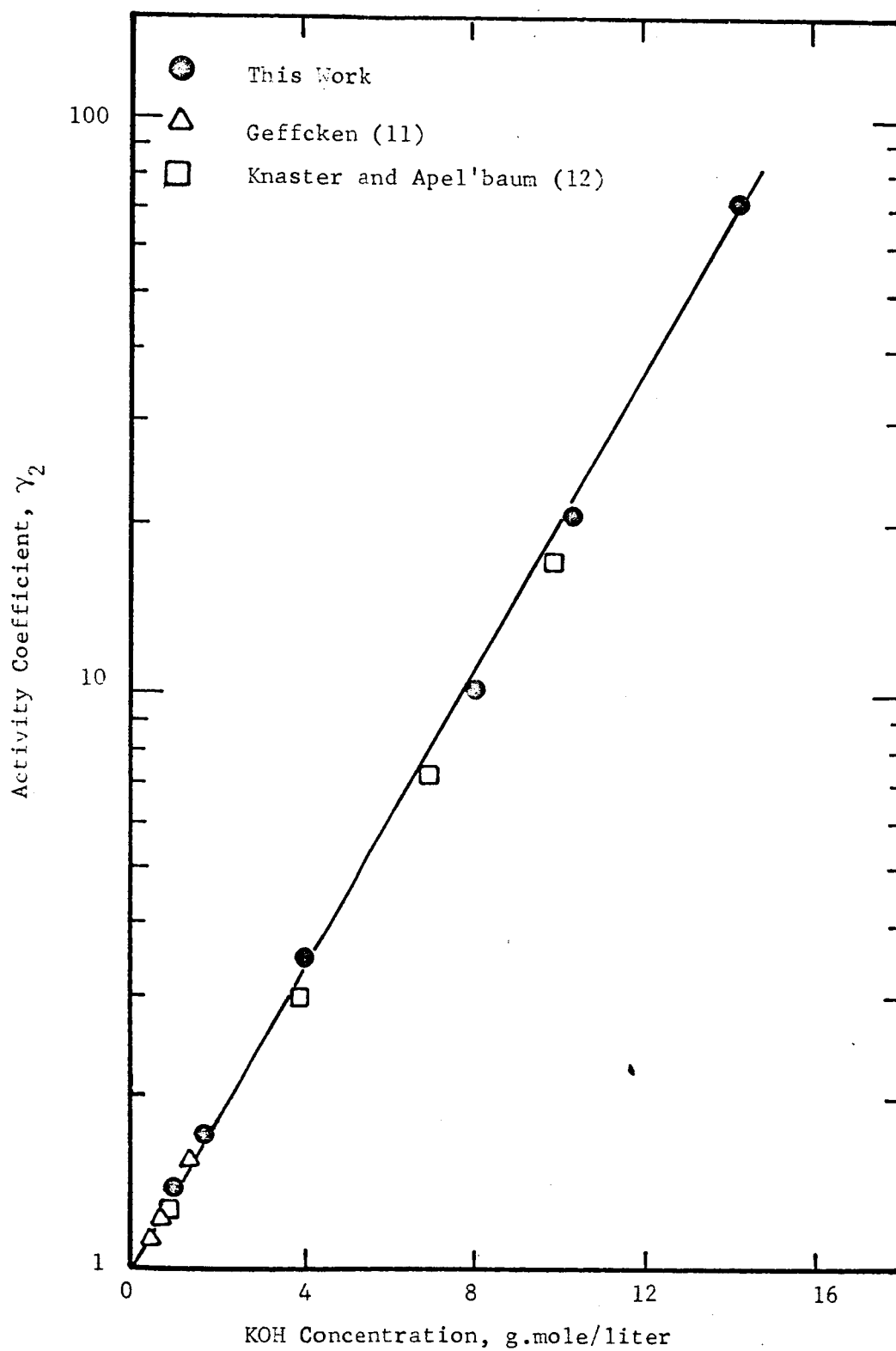


Figure 2.3-1 Activity Coefficients of Hydrogen at 25°C

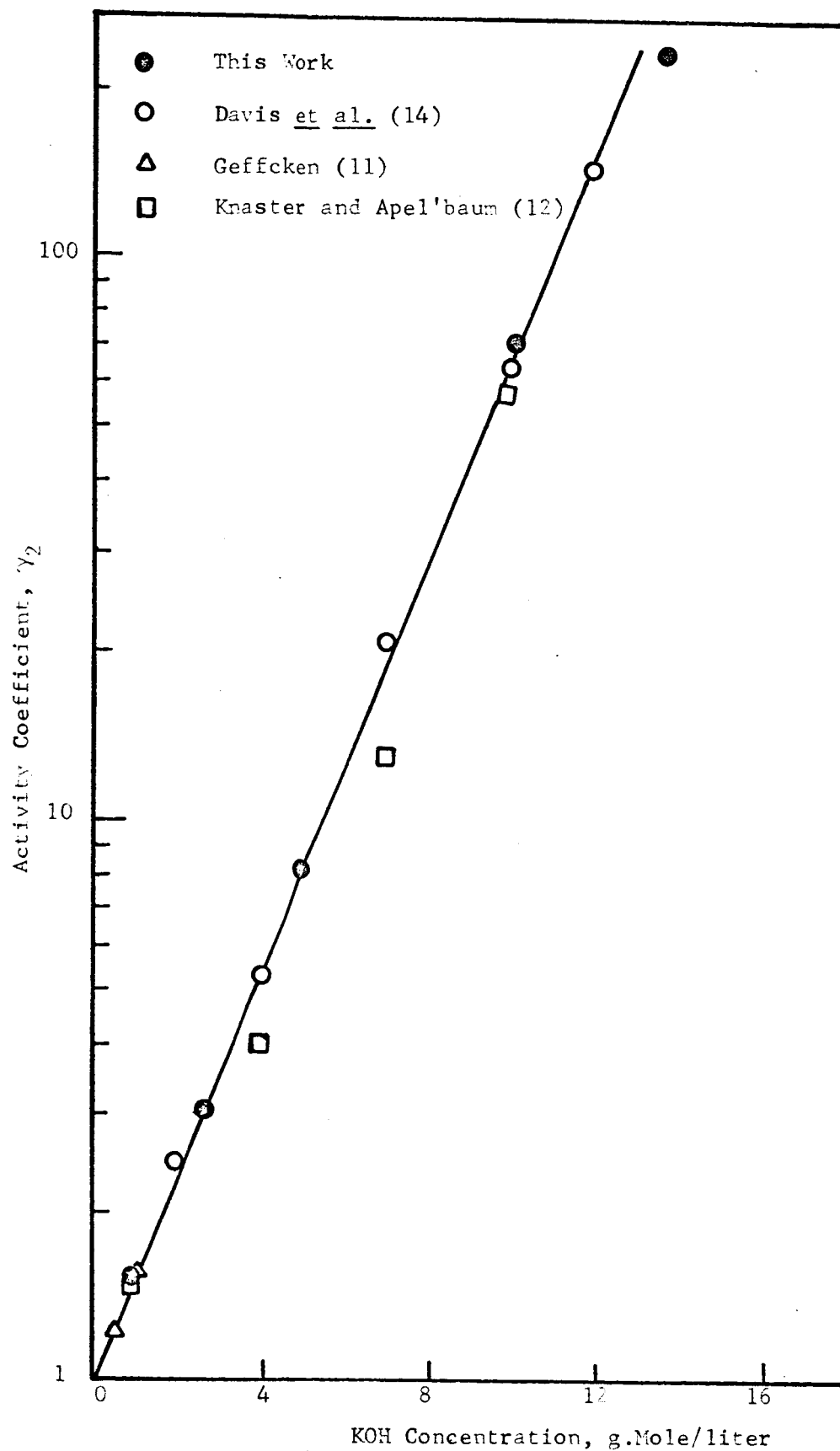


Figure 2.3-2. Activity Coefficients of Oxygen at 25°C.



Figure 2.3-1 shows that hydrogen solubilities obtained in this work at 25°C are in fairly good agreement with those of other workers. Agreement with the results of Geffcken (11) is within 2% and with those of Knaster and Apel'baum (12) is within 10%. For dilute KOH solutions, the reported results agree within 3% with those of Ruetschi and Amlie (13). However, the values of activity coefficients obtained by them are consistently lower than those reported here, and these discrepancies are as large as 10% for the higher KOH concentrations. At temperatures of 40 and 60°C, the disagreement between the reported results and those of Knaster and Apel'baum (12) is also within 10%.

Figure 2.3-2 reveals that the 25°C oxygen solubility values obtained in this work agree within 2% and 5% with those obtained by Geffcken (11) and Davis et al. (14), respectively. The experimental results of these investigators are distributed on both sides of the solid line of Figure 2.3-2. The agreement with the results of Knaster and Apel'baum (12) is quite good at very low and very high concentrations; however, at intermediate concentrations the disagreement is quite marked, the results of Knaster and Apel'baum falling consistently below the solid line. At temperatures other than 25°C, the values reported for oxygen by various workers differ appreciably, the disagreement being quite pronounced even at low potassium hydroxide concentrations. For example, the solubility value reported by Davis et al. (14) in pure water at 60°C differs by about 20% from the currently accepted literature value (15) and this suggests that discrepancies may be present at other concentrations also. The agreement of the results reported here with those of Knaster and Apel'baum (12) at 40 and 60°C is of the same general nature as at 25°C.

## 2.4 Test of Scaled Particle Theory

The scaled particle theory was used to calculate theoretical values for the solubility of various gases in potassium hydroxide solutions. The following equations developed earlier are used to make these calculations

$$\ln(\gamma_{\alpha} K_{\alpha}) = \frac{-h}{kT} g_{\alpha} + \frac{-s}{kT} g_{\alpha} + \ln\left(\frac{RT}{V} \sum n_j\right) \quad (2.1-14)$$

$$\begin{aligned} \frac{-h}{kT} g_{\alpha} = & -\ln(1-\zeta_3) + \frac{6\zeta_2}{1-\zeta_3} \left(\frac{a_{\alpha}}{2}\right) + \left[ \frac{12\zeta_1}{1-\zeta_3} + \frac{18\zeta_2^2}{(1-\zeta_3)^2} \right] \left(\frac{a_{\alpha}}{2}\right)^2 \\ & + \frac{4}{3}\pi \frac{p}{kT} \left(\frac{a_{\alpha}}{2}\right)^3 \end{aligned} \quad (2.1-19)$$

where  $\zeta_1 = \frac{\pi}{6} \sum_j (a_j)^1 \rho_j$

$$\frac{-s}{e_{\alpha}} = \frac{-s}{g_{\alpha}} = -\frac{32}{9} \pi \sum_{j=1}^3 \rho_j \epsilon_{\alpha j} \sigma_{\alpha j}^3 - \frac{4\pi \rho_1 p_{\alpha} \mu_1^2}{3\sigma_{\alpha 1}^3} \quad (2.1-26)$$

Evaluation of the free energy of making the cavity,  $\frac{-h}{g_{\alpha}}$  requires a knowledge of hard sphere diameters and density of the solvent (potassium hydroxide solutions). The densities of potassium hydroxide solutions were obtained from the literature (8,9). The hard sphere diameters of the various species were computed as shown below.

### Calculation of $\sigma$ for water

The value of  $\sigma$  for water was obtained by Pierotti (7) by the following procedure. Since  $\frac{-s}{g_{\alpha}}$  is related to the polarizability of the solute molecules (Equation 2.1-26; it will be shown later that the first term of this equation is also related to polarizability), a plot of experimental values of  $\ln(\gamma_{\alpha} K_{\alpha})$  against the polarizability,  $p_{\alpha}$ , of

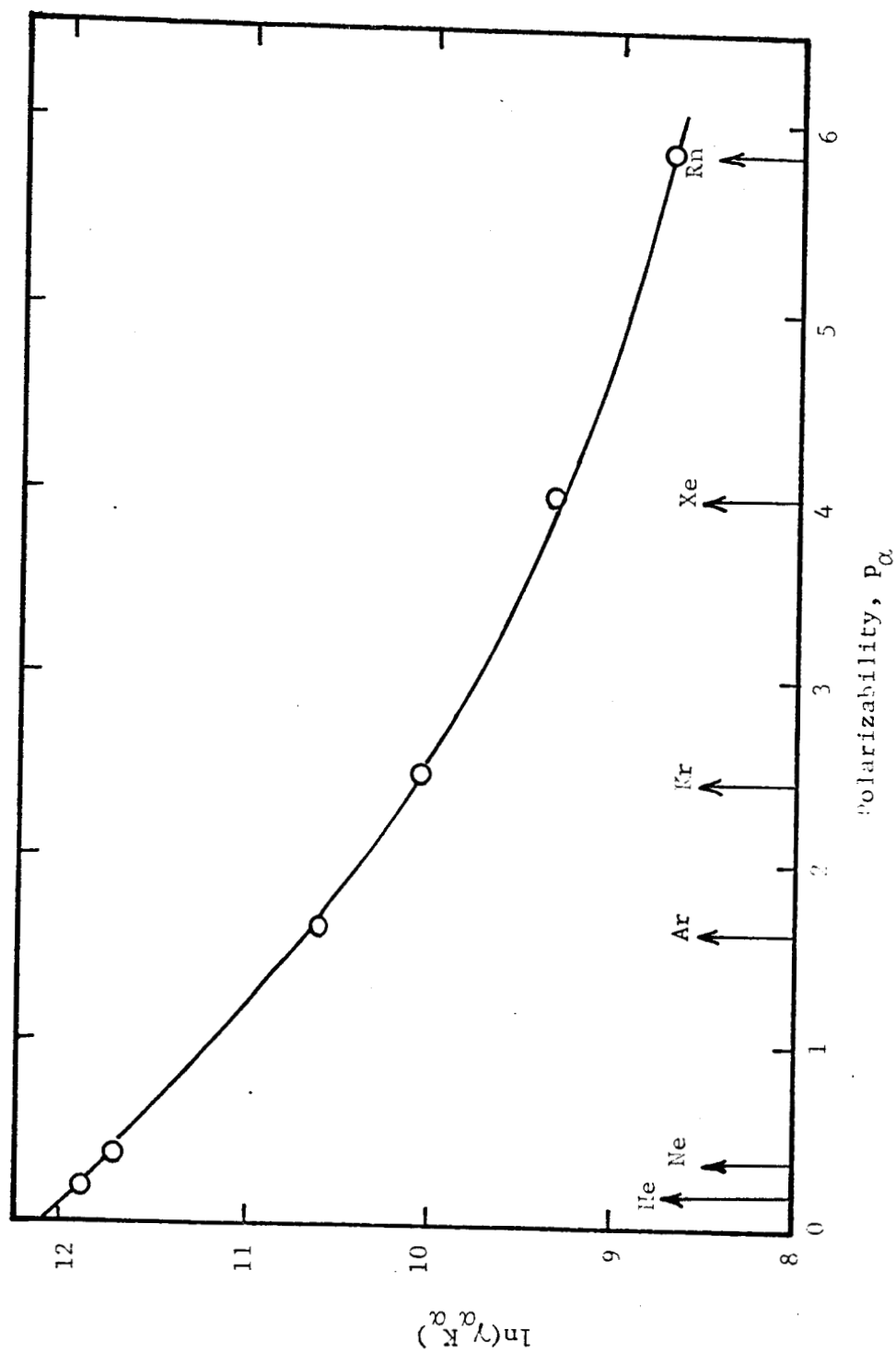


Figure 2.4-1 Experimental  $\ln(\gamma_K^\alpha)$  vs. Polarizability for Solubility of Rare Gases in Water at 25°C

spherical solutes (the rare gases) should be a smooth curve. Figure 2.4-1 shows such a plot for the solubility of rare gases in water. It was shown by Pierotti (6) that the extrapolation of such a curve to zero polarizability was equivalent to obtaining the solubility of a hard sphere of diameter  $2.58 \text{ \AA}$ . This was expressed as:

$$\lim_{p_{\alpha} \rightarrow 0} \ln(\gamma_{\alpha} K_{\alpha})^0 = \frac{-h}{kT} + \ln\left(\frac{RT}{V} \sum n_j\right) \quad (2.4-1)$$

$$p_{\alpha} \rightarrow 0$$

$$\sigma_{\alpha} \rightarrow 2.58 \text{ \AA}$$

where  $(\gamma_{\alpha} K_{\alpha})^0$  is the Henry's Law constant for a hypothetical solute having a hard sphere diameter of  $2.58 \text{ \AA}$ . Thus  $\sigma$  for water was calculated by means of Equation 2.4-1 using a value of  $2.58 \text{ \AA}$  for  $\sigma_{\alpha}$  and the experimental value of  $(\gamma_{\alpha} K_{\alpha})^0$  at  $25^{\circ}\text{C}$ . This value is shown in Table 2.4-1. It may be pointed out that  $\sigma$  calculated by the above procedure will vary somewhat with temperature. However, initially results will be calculated using the constant  $\sigma$  calculated above ( $25^{\circ}\text{C}$ ), and the temperature dependence of  $\sigma$  will be discussed later.

#### $\sigma$ for Ions

This parameter is not available in the literature. It seems appropriate, however, to take  $\sigma$  as twice the value of crystal radius of the ion. Since crystal radii of ions are difficult to determine, there is considerable disagreement between the values reported by various workers. For this reason  $\sigma$  values for  $\text{K}^{+}$  and  $\text{OH}^{-}$  were obtained as follows: Equation 2.4-1 was written for 10 and 20% KOH solution at  $25^{\circ}\text{C}$  and then, by using  $\sigma_{\text{H}_2\text{O}}$  as calculated earlier and  $\sigma_{\alpha}$  as  $2.58 \text{ \AA}$ , these

two equations were solved simultaneously to obtain  $\sigma$  for  $K^+$  and  $OH^-$ . It may be noted that these equations were not solved in a rigorous manner but by a trial and error procedure using  $\sigma$  for ions in the first trial as twice the value of crystal radii. The values obtained are listed in Table 2.4-1. As in the case of water, the ionic diameter  $\sigma$  obtained by the above procedure varies with temperature. These variations will be discussed later. The values of  $\frac{\sigma}{2}$  for ions as obtained above are quite different from hydration radii. In addition the value of  $\frac{\sigma}{2}$  for the hydroxyl ion,  $1.30 \text{ \AA}$  is much larger than the value  $0.46 \text{ \AA}$  obtained from ionic mobility measurements. The abnormally low value of the radius calculated from ionic mobility for the hydroxyl ion is due to the special mobility ("proton-jump") mechanism of these ions. This mechanism was discussed by Bernal and Fowler (19).

#### $\sigma$ for Solute Gases

The values of  $\sigma$  for solute gases were obtained from reference (22) and were the same as used by Pierotti (6). They had been calculated from second virial coefficients and are tabulated in Table 2.4-2.

Calculation of the free energy of introducing the solute molecule into the cavity,  $\bar{g}_\alpha^s$ , by means of Equation 2.1-26 requires a knowledge of the energy parameters,  $\epsilon/k$  for all the species involved.

#### $\epsilon/k$ for Water

No single best value of  $\epsilon/k$  for water can be found in the literature. Values ranging from  $167^\circ K$  to  $775^\circ K$  have been reported (6), but none of these seem consistent. Pierotti (6) obtained the value of  $\epsilon/k$  for water from the solubility of various gases in water, using Equation

TABLE 2.4-1  
PROPERTIES AND PARAMETERS FOR SOLVENT SPECIES

Solvent Species	Parameter $\sigma, \text{\AA}$	Polarizability $p \times 10^{24} \text{ cm.}^3$	Parameter $\epsilon/k, ^\circ\text{K}$	Dipole Moment $\mu, \text{Debye}$
H <sub>2</sub> O	2.75 <sup>(a)</sup>	-	85.3 <sup>(b)</sup>	1.84
K <sup>+</sup>	2.60 <sup>(b)</sup>	0.835 <sup>(c)</sup>	239 <sup>(b)</sup>	-
OH <sup>-</sup>	3.30 <sup>(b)</sup>	1.83 <sup>(b)</sup>	137.2 <sup>(b)</sup>	-

(a) Reference 7                      (b) Calculated in this work  
(c) Reference 20

TABLE 2.4-2  
PROPERTIES AND PARAMETERS FOR THE SOLUTES

Solute	Parameter $\sigma, \text{\AA}$	Parameter $\epsilon/k, ^\circ\text{K}$	Polarizability $p \times 10^{24} \text{ cm.}^3$
Hard Sphere	2.58	0	0
He	2.63	6.03	0.204
H <sub>2</sub>	2.87	29.2	0.802
Ar	3.40	122	1.63
O <sub>2</sub>	3.46	118	1.57
CH <sub>4</sub>	3.82	137	2.70
SF <sub>6</sub>	5.51	200.9	6.21 <sup>(a)</sup>
neo-C <sub>5</sub> H <sub>12</sub>	7.44	232.5 <sup>(b)</sup>	10.36 <sup>(b)</sup>

(a) Reference 20                      (b) Reference 21

All other parameters have been obtained from  
Reference 23

2.1-14. Since we are using the same general theory as Pierotti, the same value of  $\epsilon/k$  for water will be used. This value is shown in Table 2.4-1.

#### $\epsilon/k$ for Ions

The parameter  $\epsilon/k$  for ions does not seem to have been reported in the literature. However, it is possible to estimate this parameter from various theories of dispersion interactions (24,25). The theories of London and Mavroyannis-Stephen are commonly used for this purpose. According to the London theory

$$u_{\alpha j}^d = \frac{-3}{2} \frac{p_{\alpha} p_j I_{\alpha} I_j}{I_{\alpha} + I_j} \left( \frac{1}{r^6} \right) \quad (2.4-2)$$

where  $u_{\alpha j}^d$  is the dispersion interaction between the solute molecule and the solvent species  $j$ .  $I_{\alpha}$  and  $I_j$  are ionization potentials of solute and solvent species, respectively. According to the Mavroyannis-Stephen theory

$$u_{\alpha j}^d = \frac{-3}{2} \frac{a_0^{\frac{1}{2}} e^2 \bar{p}_{\alpha} \bar{p}_j}{\left( \frac{\bar{p}_{\alpha}}{Z_{\alpha}} \right)^{\frac{1}{2}} + \left( \frac{\bar{p}_j}{Z_j} \right)^{\frac{1}{2}}} \left( \frac{1}{r^6} \right) \quad (2.4-3)$$

where  $\bar{p}_{\alpha}$  and  $\bar{p}_j$  are respectively the polarizabilities of species  $\alpha$  and  $j$  in the mixture.  $Z$  is the total number of electrons in a particle,  $a_0$  is the Bohr radius and is equal to  $0.5292 \text{ \AA}^0$ , and  $e$  is electronic charge.

The dispersion interaction from the Lennard-Jones 6-12 potential is

$$u_{\alpha j}^d = -4\epsilon_{\alpha j} \sigma_{\alpha j}^6 \left( \frac{1}{r^6} \right) \quad (2.4-4)$$

On comparing Equations 2.4-2 and 2.4-4, and Equations 2.4-3 and 2.4-4, we obtain

$$4\epsilon_{\alpha j} \sigma_{\alpha j}^6 = \frac{3}{2} p_{\alpha} p_j \frac{I_{\alpha} I_j}{I_{\alpha} + I_j} \quad (\text{London}) \quad (2.4-5)$$

and

$$4\epsilon_{\alpha j} \sigma_{\alpha j}^6 = \frac{3}{2} \frac{a_o e^2 \bar{p}_{\alpha} \bar{p}_j}{\left(\frac{\bar{p}_{\alpha}}{Z_{\alpha}}\right) + \left(\frac{\bar{p}_j}{Z_j}\right)} \quad (\text{Mavroyannis-Stephen}) \quad (2.4-6)$$

For like-pair interactions, these equations become

$$4\epsilon_{\sigma}^6 = \frac{3}{4} p^2 \quad (\text{London}) \quad (2.4-7)$$

$$4\epsilon_{\sigma}^6 = \frac{3}{4} a_o^{\frac{1}{2}} e^2 p_{\alpha}^{3/2} Z^{\frac{1}{2}} \quad (\text{Mavroyannis-Stephen}) \quad (2.4-8)$$

To compare the validity of the above dispersion theories, Equations 2.4-7 and 2.4-8 were used to calculate  $\epsilon/k$  parameter for molecules such as  $O_2$ , Ar, etc. London's theory was found to yield values which were much smaller than those commonly reported in the literature (22). On the other hand the values calculated by the Mavroyannis-Stephen theory were in very good agreement with literature values. According to Reed (24), for monatomic gases, the Mavroyannis-Stephen expressions reproduce the empirical parameter  $\epsilon/k$  quite accurately. Thus, in this work Equation 2.4-8 is used to calculate  $\epsilon$  for ions. After substitution of the values of  $a_o$  and  $e$  this equation can be written as

$$\epsilon = \frac{3.146 \times 10^{-12} p_{\alpha}^{3/2} Z^{1/2}}{\sigma^6} \quad (2.4-9)$$

To calculate  $\epsilon$  for  $K^+$  and  $OH^-$  by means of the above equation, we need the polarizability,  $p_{\alpha}$  of these ions. The polarizabilities of



most ions have been tabulated in the Landolt-Bornstein Tables (20). However, the polarizability of  $\text{OH}^-$  was not available in the literature, and was calculated from molar refraction data by the following procedure (26,27):

The energy quantity corresponding to the second order Stark effect of a system is

$$\Delta E = -\frac{1}{2} p \epsilon^2,$$

and the electric moment induced in the system is

$$\mu^{(\text{ind})} = p\epsilon$$

The polarization,  $P$  in unit volume can be expressed in terms of the index of refraction  $n$  as

$$P = \frac{\tilde{N}}{V} \mu^{(\text{ind})} = \frac{\tilde{N}}{V} p\epsilon = \frac{3}{4\pi} \frac{n^2-1}{n^2+2} \epsilon \quad (2.4-10)$$

The molar refraction  $R$  is defined by the equation

$$R = V \frac{n^2-1}{n^2+2} = \frac{4\pi\tilde{N}}{3} p \quad (2.4-11)$$

or

$$p = \frac{3R}{4\pi\tilde{N}} = \frac{R}{2.54} \times 10^{-24} \text{ cm}^3 \quad (2.4-12)$$

Molar refraction data for  $\text{OH}^-$  were obtained from reference (19). The polarizability value of  $\text{OH}^-$  calculated by the above procedure is shown in Table 2.4-1. Also included in this table are  $\epsilon/k$  parameters for  $\text{K}^+$  and  $\text{OH}^-$  calculated by means of Equation (2.4-9).

#### $\epsilon/k$ for Solute Gases

For most of the solute gases  $\epsilon/k$  parameters were obtained from the compilation of Hirschfelder, Curtiss and Bird (23). These authors

have listed Lennard-Jones parameters obtained from second virial coefficient and viscosity data. The former were used in this work. These parameters together with the polarizabilities of the solute gases have been tabulated in Table 2.4-2.

The values of  $\ln(\gamma_{\alpha} K_{\alpha})$  for various solutes calculated by scaled particle theory are compared with experimental values in Table 2.4-3. It is seen that at 25°C, the agreement is very good except in the case of large molecules like  $\text{SF}_6$  and neo- $\text{C}_5\text{H}_{12}$ . In most cases the agreement between the theoretical and experimental values of the quantity  $\gamma_{\alpha} K_{\alpha}$  (inversely proportional to solubility) is better than 15%. In the case of  $\text{SF}_6$  and neo- $\text{C}_5\text{H}_{12}$ , it should be noted that the theoretical values of  $\ln(\gamma_{\alpha} K_{\alpha})$  for the solubility of these gases in water are lower and higher, respectively, than the corresponding experimental quantities. This trend continues even for potassium hydroxide solutions. A possible explanation for these discrepancies may be as follows: Firstly, since the Lennard-Jones parameters,  $\sigma$  and  $\epsilon/k$ , are not known accurately for various substances, they might be significantly in error for these large molecules. Since the calculated values are very sensitive to  $\sigma$  values, a small error in this parameter can result in an appreciable error in  $\ln(\gamma_{\alpha} K_{\alpha})$ . Secondly, the various assumptions involved in the theory might not be justified for these systems. These assumptions are discussed below.

It should be recalled that the only assumptions involved in the calculation of the free energy of making the cavity,  $\bar{g}_{\alpha}^h$  are that (i) the molecules are composed of an inner hard core and an outer soft part, (ii) the hard core diameter is temperature independent. By

TABLE 2.4-3  
Comparison of Theoretical and Experimental

VALUES OF  $\ln(\gamma_{\alpha}^{K_{\alpha}})$

25°C

Gas	0% KOH		10%		20%		30%		40%		50%	
	Expt.	Theo.	Expt.	Theo.	Expt.	Theo.	Expt.	Theo.	Expt.	Theo.	Expt.	Theo.
He	11.86	11.62	12.25	11.98	13.10	12.85	14.05	13.62	-	-	-	-
H <sub>2</sub>	11.17	11.10	11.85	12.36	12.41	12.53	13.17	13.42	-	-	15.2	16.15
Ar	10.62	10.34	11.38	10.97	12.30	11.90	-	-	14.58	14.16	-	-
O <sub>2</sub>	10.66	10.51	11.50	11.33	12.46	12.22	13.54	13.20	-	-	16.07	16.20
CH <sub>4</sub>	10.58	10.58	11.46	11.38	12.49	12.48	-	-	15.10	15.17	-	-
SF <sub>6</sub>	12.38	10.75	13.88	12.38	15.58	14.10	17.52	16.25	-	-	-	-
neo-C <sub>5</sub> H <sub>12</sub>	11.51	11.80	12.99	13.55	14.81	16.43	16.85	19.87	-	-	-	-

80°C

He	11.74	11.42	12.39	12.11	13.18	12.83	14.10	13.71	-	-	-	-
H <sub>2</sub>	11.24	10.67	11.90	11.89	12.55	12.67	13.28	13.62	-	-	15.29	16.03
Ar	11.10	10.81	11.75	11.56	12.55	12.44	-	-	14.60	14.72	-	-
O <sub>2</sub>	11.13	11.04	11.81	11.72	12.68	12.66	13.63	13.83	-	-	16.07	16.82
CH <sub>4</sub>	11.14	11.18	11.86	12.05	12.70	13.10	-	-	14.80	15.79	-	-
SF <sub>6</sub>	13.17	12.49	14.30	13.99	15.72	15.79	17.36	18.10	-	-	-	-
neo-C <sub>5</sub> H <sub>12</sub>	12.37	14.42	13.61	16.43	15.15	19.40	16.91	23.10	-	-	-	-

calculating the solubility of a hard sphere solute of diameter  $2.58 \text{ \AA}$  in various solvents Pierotti (6) has shown that these assumptions cause little error at  $25^\circ\text{C}$ . The following assumptions were made in the calculation of the free energy of introducing the molecule into the cavity  $\bar{g}_\alpha^s$ .

(i) The  $\bar{p}v_\alpha^s$  contribution to the free energy is assumed negligible. It has been shown by Pierotti (6) that  $\bar{v}_\alpha^s$  is a small negative number for weakly interacting solutes, and should become larger as the interaction energy increases. Since we are concerned with a pressure of the order of only one atmosphere, neglecting  $\bar{p}v_\alpha^s$  should cause a negligible error.

(ii) The second assumption was that  $\bar{T}s_\alpha^s$  can be neglected as compared to  $\bar{e}_\alpha^s$ . It is difficult to determine this quantity, but it is known that  $\bar{s}_\alpha^s$  will be negative. Since the system becomes more organized if the interaction energy is large,  $\bar{T}s_\alpha^s$  will make a significant contribution for strongly interacting solutes. For most of the solutes considered, the interaction energies are not large and therefore neglecting  $\bar{T}s_\alpha^s$  should not cause a very significant error. However, for  $\text{SF}_6$  and neo- $\text{C}_5\text{H}_{12}$  these energies are quite high and appreciable error may arise from neglecting  $\bar{T}s_\alpha^s$ .

(iii) The third assumption which was made in the calculation of  $\bar{g}_\alpha^s$  was that the radial distribution functions  $g_{\alpha j}(r)$  are equal to unity for  $r > a_{\alpha j}$ . Since  $g_{\alpha j}(r)$  is a function of the interaction energies, this assumption should not be very good for strongly interacting molecules like  $\text{SF}_6$  and neo- $\text{C}_5\text{H}_{12}$ . For such molecules the solvent species

cannot be uniformly distributed around the solute, and some function should be assumed for  $g_{\alpha j}(r)$ .

(iv) The fourth factor which seems likely to be a cause of discrepancies is the form of the nonpolar pair-potential assumed. The Lennard-Jones potential was assumed to hold for all nonpolar interactions. However, for molecules such as  $\text{SF}_6$  and neopentane the pair interaction might not be adequately described by this potential.

#### Predicted Concentration Dependence.

From Table 2.4-3, it is seen that the concentration dependence of the solubility of various gases in potassium hydroxide solutions is predicted quite accurately, except for very large molecules such as neo- $\text{C}_5\text{H}_{12}$ . The main factors which might be the cause of the discrepancies in the case of large molecules have already been discussed. In all cases, both the predicted and experimental values of  $\ln(\gamma_{\alpha} K_{\alpha})$  increase with increase in potassium hydroxide concentration. To facilitate the discussion of the concentration dependence of the solubility, the experimental and calculated values of  $\ln(\gamma_{\alpha} K_{\alpha})$  for the solubility of oxygen have been plotted versus potassium hydroxide concentration in Figure 2.4-2. (The agreement between theory and experiment for this system is neither the best nor worst for the system studied.)

Results predicted by the electrostatic theories of Debye-McAulay (28) and Conway (2) are also included in this figure. It is seen that the scaled particle theory gives very good agreement for the concentration dependence. The calculated values are slightly lower than the experimental values for low and moderate potassium hydroxide

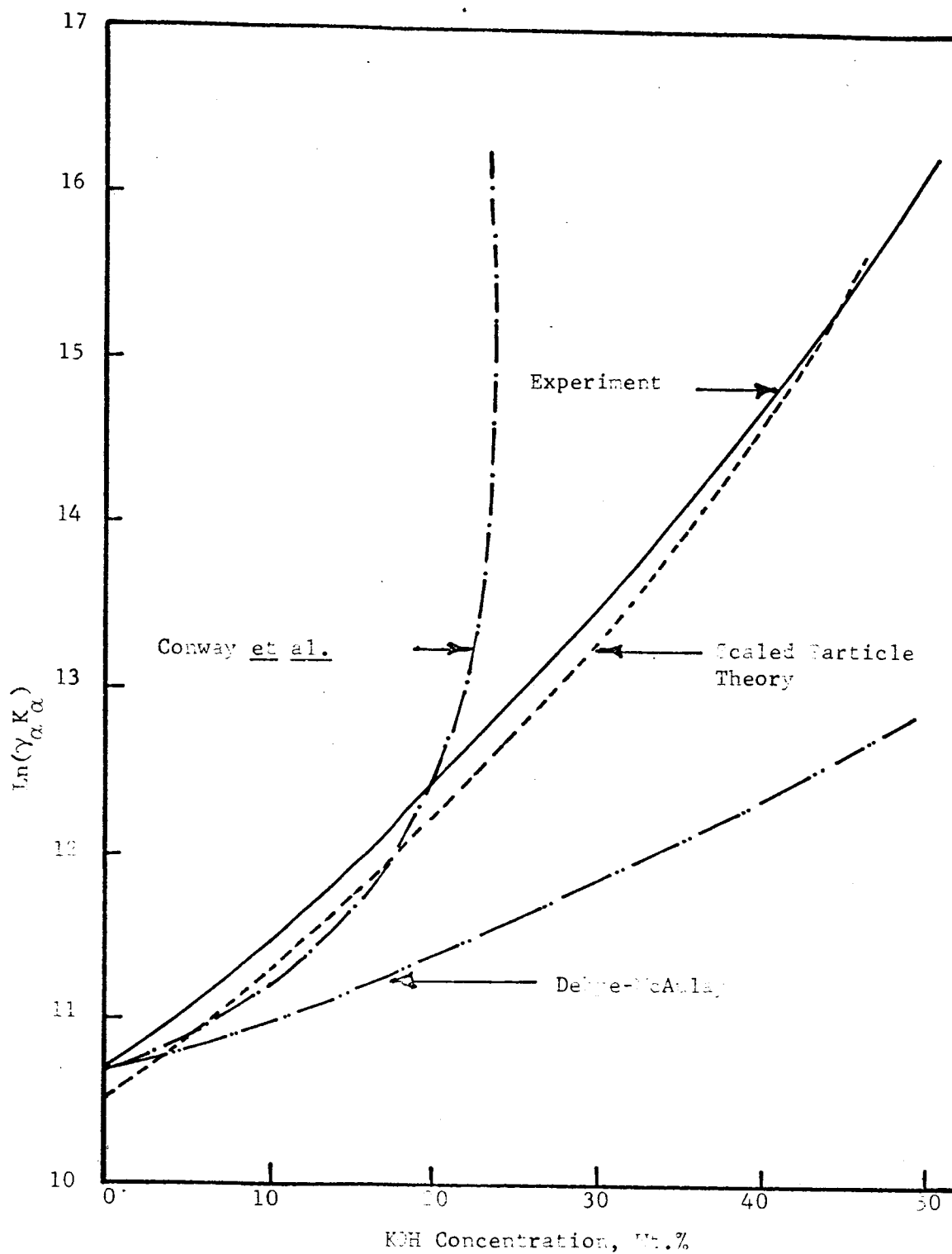


Figure 2.4-2. Theoretical and Experimental Activity Coefficients of Oxygen at 25°C.

concentrations, whereas at very high concentrations the predicted values are higher than the experimental values. The discrepancies in the results may be due to the assumptions discussed earlier. In addition, a small error in the choice of the parameter  $\sigma$  for the ions will introduce a large error in the results for concentrated solutions. The theory of Debye-McAulay (28) gives much lower results than the experimental values. On the other hand, the theory of Conway (2) gives fairly good results up to 20% KOH concentration. At higher concentrations, however, the expressions of Conway become invalid and predict a negative solubility.

#### Predicted Temperature Dependence

The results calculated from the scaled particle theory for the solubility of various gases at 80°C are also shown in Table 2.4-3. The agreement between the experimental and the calculated values is quite good for most of the solutes. As before, the agreement is poor for the case of SF<sub>6</sub> and neo-C<sub>5</sub>H<sub>12</sub>. To examine the temperature dependence of the solubility results for oxygen in 20% KOH have been plotted against absolute temperature in Figure 2.4-3. It is seen that the temperature dependence predicted is too large. To make a quantitative assessment of the temperature dependence, partial molal heats of solutions,  $\Delta\bar{H}_2$  were calculated, and these values for O<sub>2</sub> are tabulated in Table 2.4-4. It is seen that the absolute magnitude of the calculated values of  $\Delta\bar{H}_2$  is much higher than the experimental values. Similar discrepancies are present in case of other solutes.

The differences in calculated and the experimental values can be explained as follows: it has been mentioned earlier that the hard sphere diameter for various species is a function of temperature

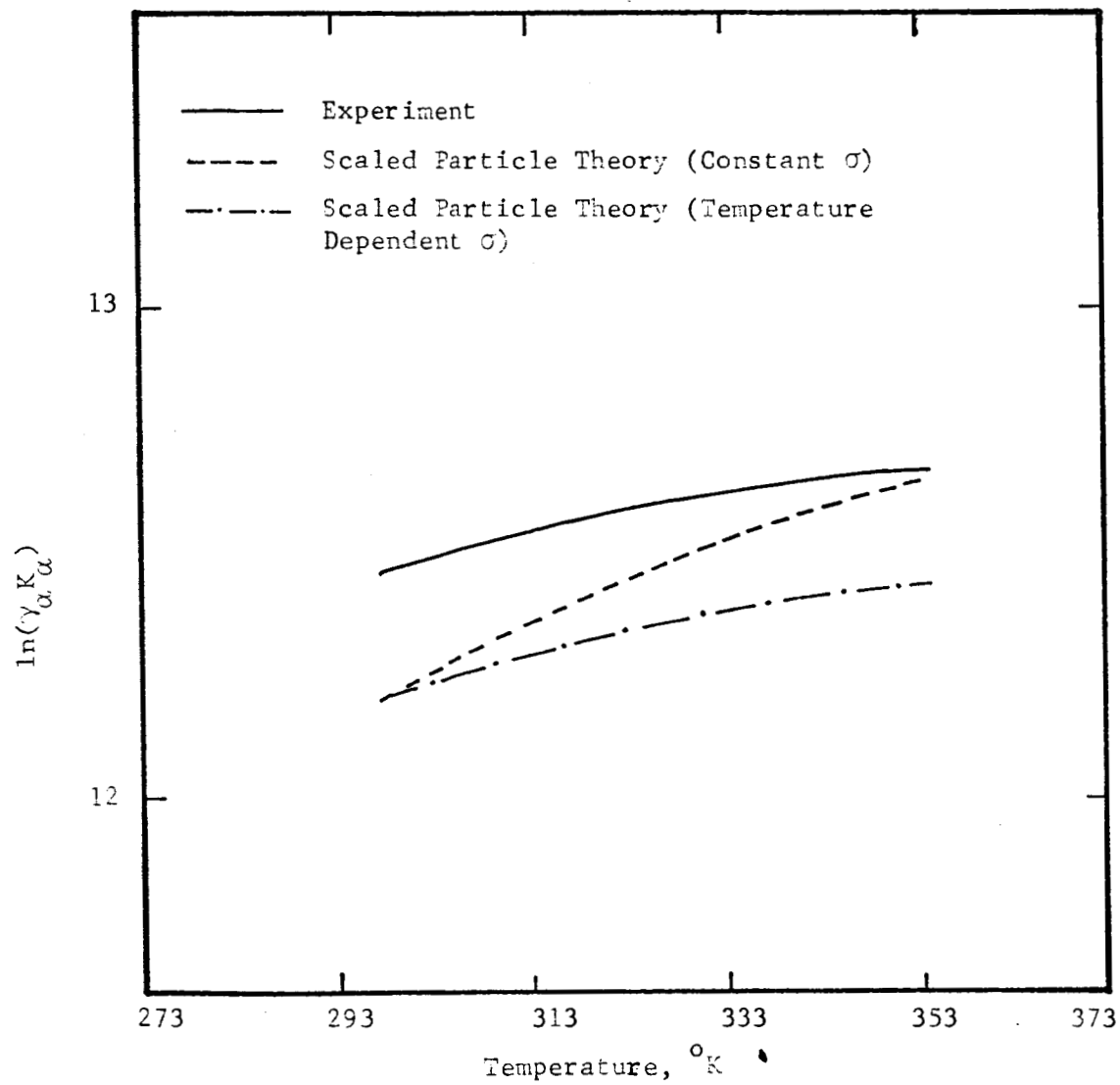


Figure 2.4-3 Effect of Temperature on Activity Coefficient of Oxygen in 20% KOH Solution



(see also references (29) and (30)). By calculating the solubility of hard spheres of diameter  $2.58 \text{ \AA}$  (zero polarizability) in water it was found that the theory predicts a decrease in the  $\sigma$  value for water (see reference 16). The value of  $\sigma$  for water obtained at  $80^\circ\text{C}$  was  $2.74 \text{ \AA}$  as against  $2.75$  at  $25^\circ\text{C}$ . This implies that  $\sigma$  for all the species involved will decrease slightly at  $80^\circ\text{C}$ . Although this decrease is very small it results in a significant error in the results. To examine the effect of the change in  $\sigma$  values at higher temperatures for various species, the solubility of  $\text{O}_2$  in 20% KOH solution was calculated by allowing  $\sigma$  to vary with temperature (see Table 2.4-5). The  $80^\circ\text{C}$  values shown for  $\sigma$  for ions and oxygen were estimated by assuming their diameters to decrease with temperature in a proportionately similar way to that of the water molecule diameter. Appropriate values of  $\sigma$  for temperatures intermediate between  $25$  and  $80^\circ\text{C}$  were obtained by interpolating between the values shown.

The results obtained are plotted in Figure 2.4-3. It is seen that these  $\sigma$  values lead to a more correct temperature dependence for the oxygen solubility. In the case of  $\text{SF}_6$  and neo- $\text{C}_5\text{H}_{12}$ , the decrease in  $\sigma$  will be still larger and will therefore introduce appreciable errors in the results at higher temperatures, as is observed in Table 2.4-3.

TABLE 2.4-4  
 $\Delta \bar{H}_2$  FOR O<sub>2</sub>/20% KOH SOLUTION, cal.(g.mole)<sup>-1</sup>

Temperature °C	Expt.	Theory
25	-1100	-2020
40	- 812	-1770
60	- 635	-1325
80	- 446	-1097

TABLE 2.4-5  
 PARAMETER  $\sigma$  FOR SOLVENT SPECIES, A°

<u>Solvent Species</u>	<u>25°C</u>	<u>80°C</u>
O <sub>2</sub>	3.46	3.45
H <sub>2</sub> O	2.75	2.74
K <sup>+</sup>	2.60	2.59
OH <sup>-</sup>	3.30	3.28

Comparison of the Electrostatic Theories and the Proposed Cavity Model  
Based on Scaled Particle Theory

(1) The most striking difference between the two principal types of theories is that whereas the Debye-McAulay and Conway theories can satisfactorily predict salting-out effects only up to 5% and 20% KOH, respectively, the proposed cavity model gives very satisfactory results for potassium hydroxide concentrations up to 50%.

(2) The electrostatic theories enable one to calculate the solubility of the solute in an electrolytic solution only if the corresponding solubility in water is known. On the other hand, the proposed cavity model gives the former quantity directly.

(3) The temperature dependence of the solubility can be fairly satisfactorily calculated by the cavity model whereas electrostatic theories cannot attempt such a calculation because the parameters needed for these theories are usually not available at higher temperatures.

(4) The proposed cavity model should be able to predict the observed salting-in phenomena in cases when the total molecular polarization of the solute is less than that of the solvent. In such cases the electrostatic theories predict that salting-out should occur. In fact, Bockris et al. (31) recognized the importance of nonpolar interactions in a solute/electrolyte system and accounted for the salting-in of benzoic acid by tetra alkyl ammonium iodides in aqueous and ethylene glycol solutions by considering Van der Waal's forces between the solute and the ions in addition to the coulombic forces.

(5) The electrostatic theories are difficult to use because the parameters involved are difficult to obtain accurately. On the other

hand, the cavity model contains parameters which are either easily available or can be calculated with adequate accuracy and without undue difficulty.

In addition to the above obvious advantages of the cavity model, based on the scaled particle theory, over electrostatic theories, there is an important conceptual advantage: The proposed model is simple, easy to visualize and starts with fairly rigorous equations of statistical mechanics. The solubility of a gaseous solute in organic solvents (6), water (7) and electrolytic solutions can be explained in terms of single theory involving no assumptions concerning the structure of the solvent. Electrostatic theories, on the other hand, start with the basically incorrect assumption of a continuous medium, are difficult to conceive, and become still more obscure when the ideas concerning the structure of the solvent, hydration shells, and dielectric saturation effect are introduced.

The proposed model raises an interesting point. The fact that the ions are charged does not appear to affect the solubility process to a significant extent. The difference between the solubility phenomena in electrolytic solutions and pure water appears to lie in the fact that the former contains a number of particles (ions) having molecular parameters which are different than those of water. The nonpolar interactions between the solute and the ions are found to be the only interactions which are important. This is in contradistinction to earlier viewpoints (1) in which the electrostatic interactions and hydration effects were supposed to be mainly responsible for salting phenomena.

### 3.0 DIFFUSION COEFFICIENTS OF OXYGEN AND HYDROGEN IN POTASSIUM HYDROXIDE SOLUTION - M. K. Tham

Measurements have been made of the diffusion coefficients of oxygen in potassium hydroxide at 25°, 40° and 60°C, and at concentrations up to saturation. Also, diffusion coefficients of H<sub>2</sub> at 25° and 40°C have been measured for the same concentration range.

Slight changes in experimental procedure have been made after the Fourth Semi-Annual Report.

#### 3.1 Experimental Procedures

##### 3.1.1 Presaturation of Gases

The oxygen and hydrogen gas used in the experiments were presaturated with water vapor by bubbling through two presaturators before introduction into the diffusion cell. The presaturators were filled with potassium hydroxide of the concentration being studied, and controlled at the same temperature as the solution being measured. An oil bath was used for controlling temperature in order to prevent any interference from other electrical instruments (inadvertent spillage of KOH has occasionally posed a few problems).

##### 3.1.2 Procedure

The oxygen or hydrogen gas, presaturated with water vapor, was bubbled through the solution in the diffusion cell for thirty to forty minutes. The gas-saturated solution was then drawn into the pretreated capillary electrode by means of a hyperdermic syringe, after which the bubbling of gas was stopped, and the solution was allowed to equilibrate with the surrounding medium for five minutes before the measurement of the current was begun. Using a Sargent Model XV recorder-polarograph, the

current-time curve was recorded for 18 to 20 minutes while applying a constant voltage. The voltage applied, which corresponds to the voltage for concentration polarization to take place, was 0.4 to 0.65V for oxygen and +0.1 to 0.2V for hydrogen with respect to a saturated calomel electrode. After each measurement, gas was again bubbled through the solution for five minutes, during which time the pretreatment procedure was repeated. Then the capillary was refilled with fresh solution, and the measurement was repeated. Five to six repetitions were made for each experiment, and the arithmetic mean of the current measured was used for calculating the diffusion coefficient by means of the following equation

$$D = \left( \frac{i}{nFCA} \right) \pi t$$

where  $i$  = current in amperes  
 $n$  = number of Faradays of electricity required per mole of electrode reaction  
 $F$  = Faraday  
 $C$  = concentration of diffusing material  
 $A$  = cross-sectional area of diffusion path  
 $t$  = time at which the current is measured

To measure the residual current, nitrogen gas was bubbled through the solution, thus stripping out the diffusing gas, after which the same procedure as that for measuring diffusion current was followed. The stripping and measuring were repeated until there were no changes in residual current for two successive measurements.

### 3.1.3. Pretreatment of Electrodes

The platinum electrode was pretreated according to the procedure suggested by Damjanovic et al. (32). Before sealing the platinum disc, it was first washed with acetone, distilled water, concentrated sulfuric acid and again with distilled water. To remove

sulfate ion, the electrode was immersed in potassium hydroxide for 15 minutes. Before each measurement, the electrode was cleaned by means of cathodic evolution of hydrogen. When measuring hydrogen diffusivity, the electrode was polarized at a potential of -0.2V vs. saturate calomel electrode for a period of 1 minute to activate the platinum (33).

### 3.2 Results and Discussion

The diffusion coefficients of  $O_2$  and  $H_2$  are tabulated in Tables 3.2-1 and 3.2-2. The deviations are standard deviations from the arithmetic mean for 5 to 6 measurements. The data are plotted against weight percent potassium hydroxide in Figures 3.2-1 and 3.2-2, and against species fraction in Figures 3.2-3 and 3.2-4. The existing data for the same system were also shown in Figures 3.2-1 and 3.2-2. The values of diffusion coefficients at 25°C are only slightly less than those of Tobias et al. (34), but those at 60°C differ significantly. This may be attributed to the difference in the value of solubilities used. (See Figure 2.1, Fourth Semi-Annual Report.)

The values of diffusion coefficients for  $H_2$  at 30°C as measured by Ruetschi (35) are quite different from the values measured in this work. No comparison can be made at this time since both the method of measurement and the solubility data (see Figure 2.2, Fourth Semi-Annual Report) are different.

In Figures 3.2-3 and 3.2-4 the values of diffusion coefficient were plotted against species fraction. According to Ratcliff (36) and K. K. Bhatia (37), all the points should be on a straight line. It can be seen that the data deviate from a straight line, especially for the

higher electrolyte concentration data, which suggests that the simple theory does not hold well for concentrated solutions.

The Eyring equation predicts that a plot of  $\ln \left( \frac{D}{T} \right)$  vs  $\frac{1}{T}$  should give a straight line. Such a plot is shown in Figure 3.2-5, which gives reasonably straight lines for various KOH concentrations; however, it should be noted that too few temperatures have been studied to give a good test of theory.



TABLE 3.2-1  
DIFFUSION COEFFICIENTS OF OXYGEN IN KOH SOLUTION

Concentration, Wt % KOH	$D \times 10^5, \text{cm.}^2/\text{sec.}$		
	25°C	40°C	60°C
3.5		2.46 $\pm$ 0.02	
5.0			3.4 $\pm$ 0.012
6.0	1.45 $\pm$ 0.018		
10.2	1.18 $\pm$ 0.02	1.75 $\pm$ 0.01	
13.0			2.45 $\pm$ 0.021
19.0	0.85 $\pm$ 0.015	1.25 $\pm$ 0.019	1.8 $\pm$ 0.016
26.0	0.6 $\pm$ 0.018	0.90 $\pm$ 0.01	
32.5			1.05 $\pm$ 0.02
40.2	0.4 $\pm$ 0.01	0.57 $\pm$ 0.02	
42.5			0.85 $\pm$ 0.01
51.5	0.3 $\pm$ 0.012	0.45 $\pm$ 0.015	0.72 $\pm$ 0.01

TABLE 3.2-2  
DIFFUSION COEFFICIENTS OF HYDROGEN IN KOH SOLUTIONS

Concentration, Wt % KOH	$D \times 10^5, \text{cm.}^2/\text{sec.}$	
	25°C	40°C
5.0	3.1 $\pm$ 0.015	4.6 $\pm$ 0.028
13.0	2.36 $\pm$ 0.02	3.6 $\pm$ 0.017
24.0	1.85 $\pm$ 0.01	2.74 $\pm$ 0.01
32.5	1.55 $\pm$ 0.023	2.4 $\pm$ 0.01
42.5	1.25 $\pm$ 0.01	1.95 $\pm$ 0.02
51.5	1.10 $\pm$ 0.01	1.8 $\pm$ 0.01

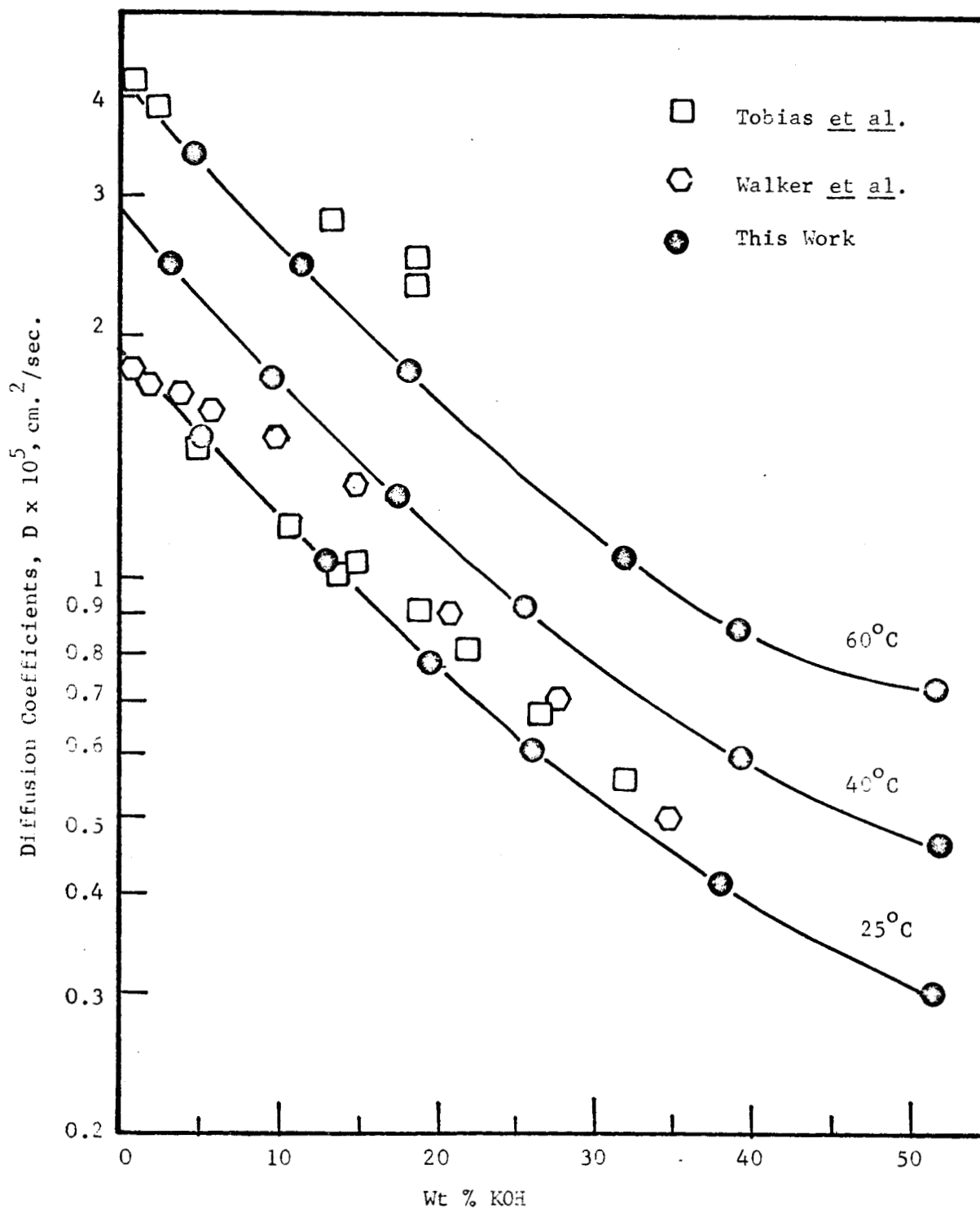


Figure 3.2-1 Diffusion Coefficients of O<sub>2</sub> in KOH Solutions

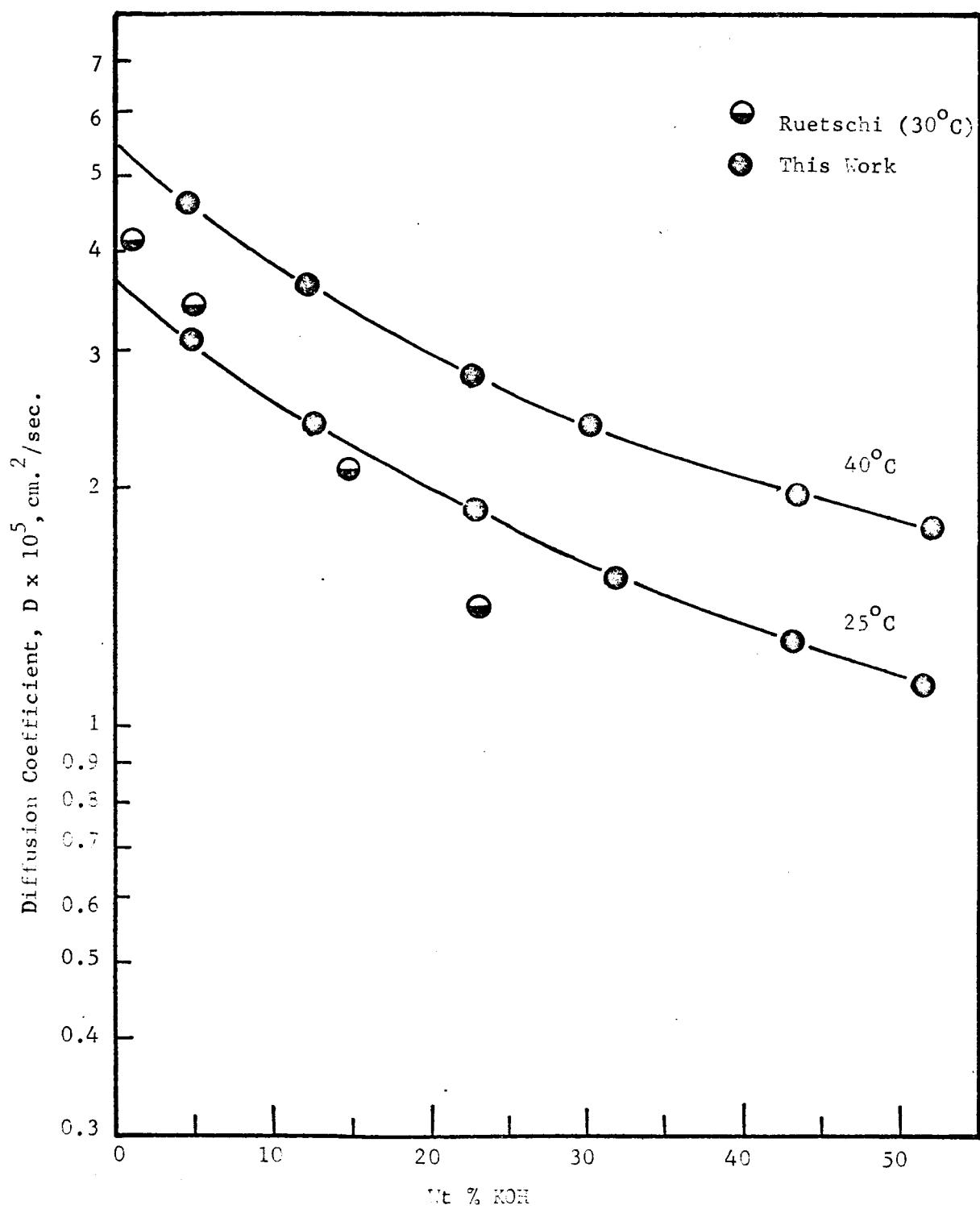


Figure 3.2-2 Diffusion Coefficient of  $\text{H}_2$  in KOH Solutions

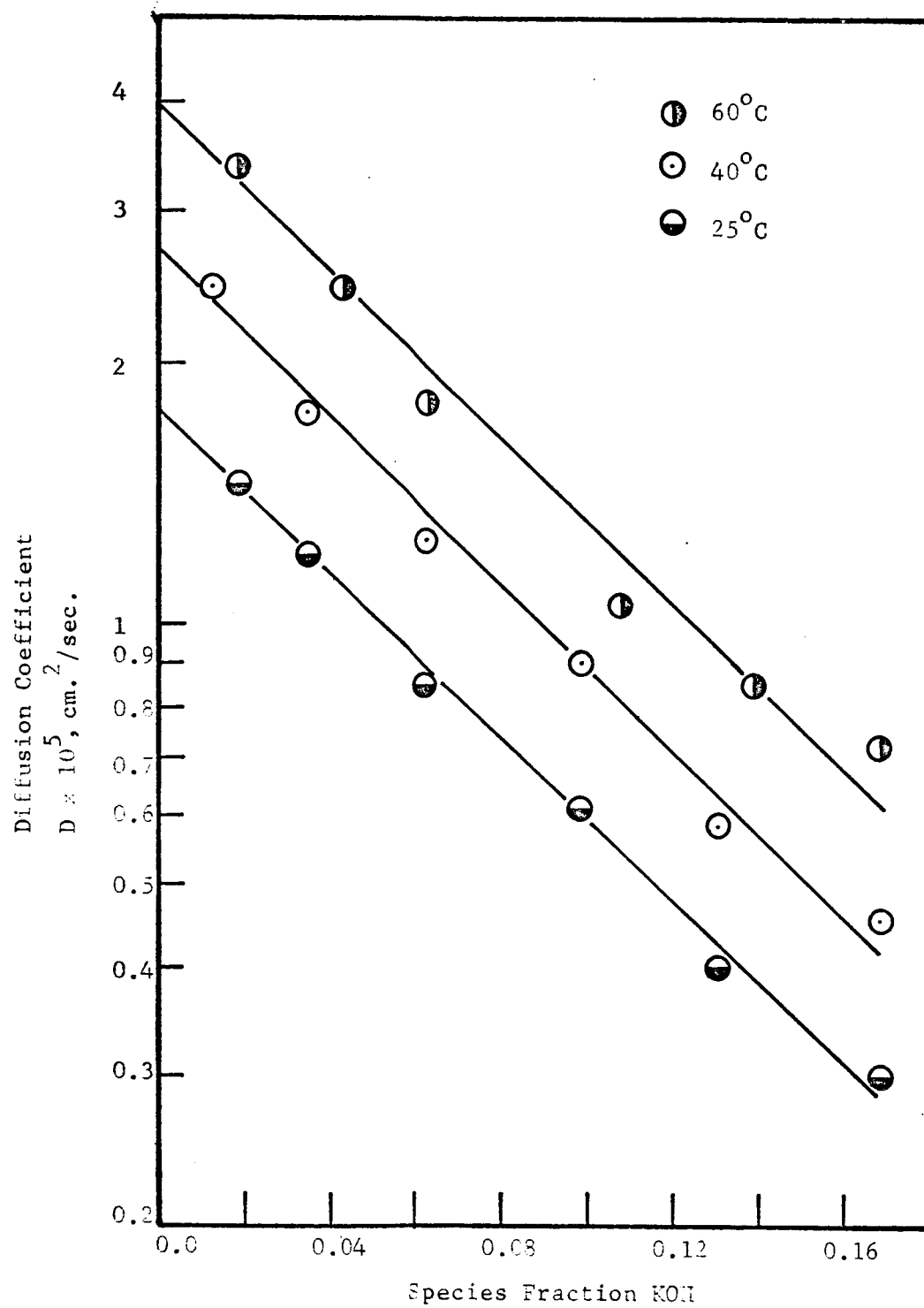


Figure 3.2-3 Diffusion Coefficient of  $\text{O}_2$  vs Species Fraction of KOH

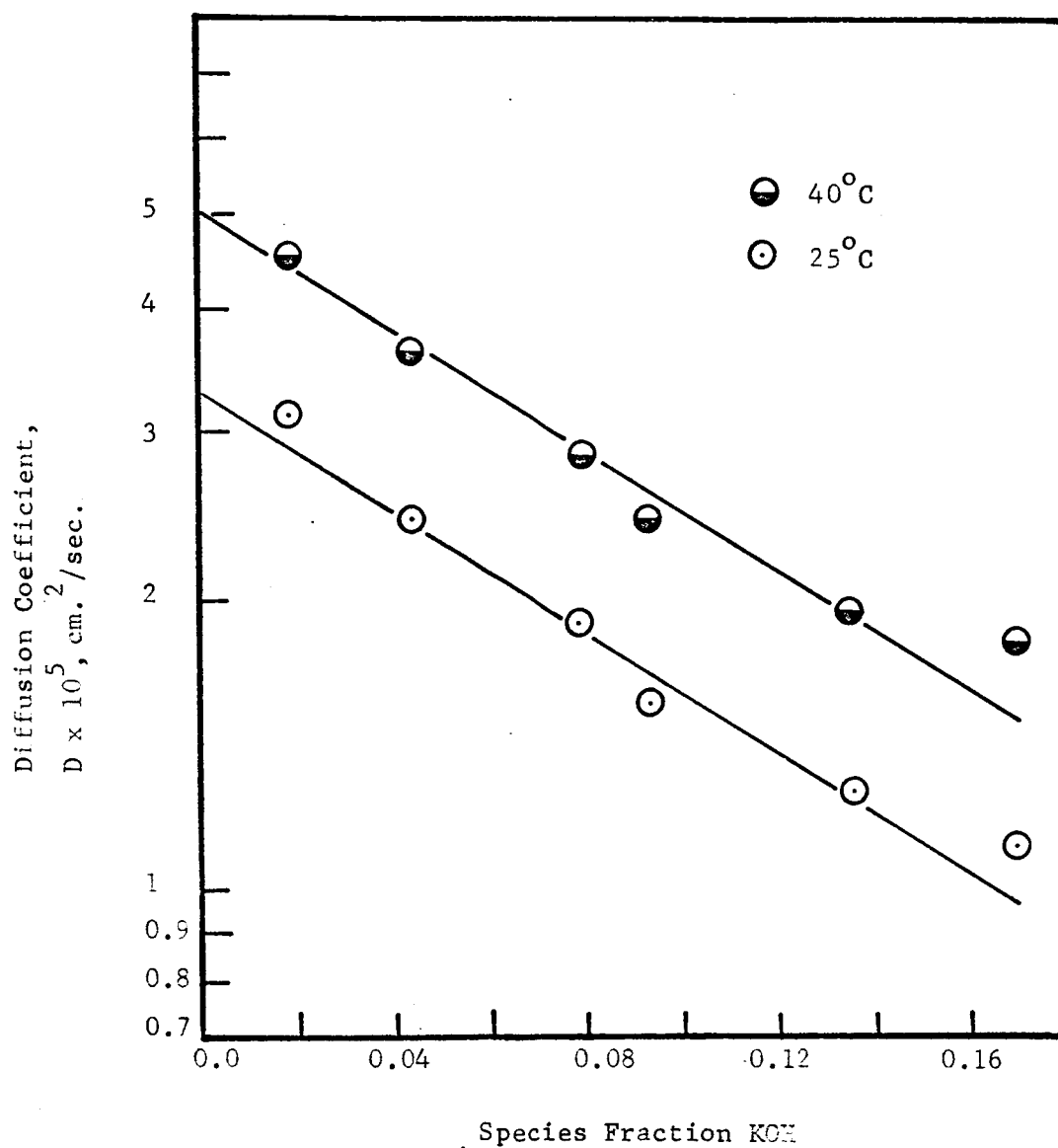


Figure 3.2-4 Diffusion Coefficients of  $\text{H}_2$  vs Species Fraction of KOH

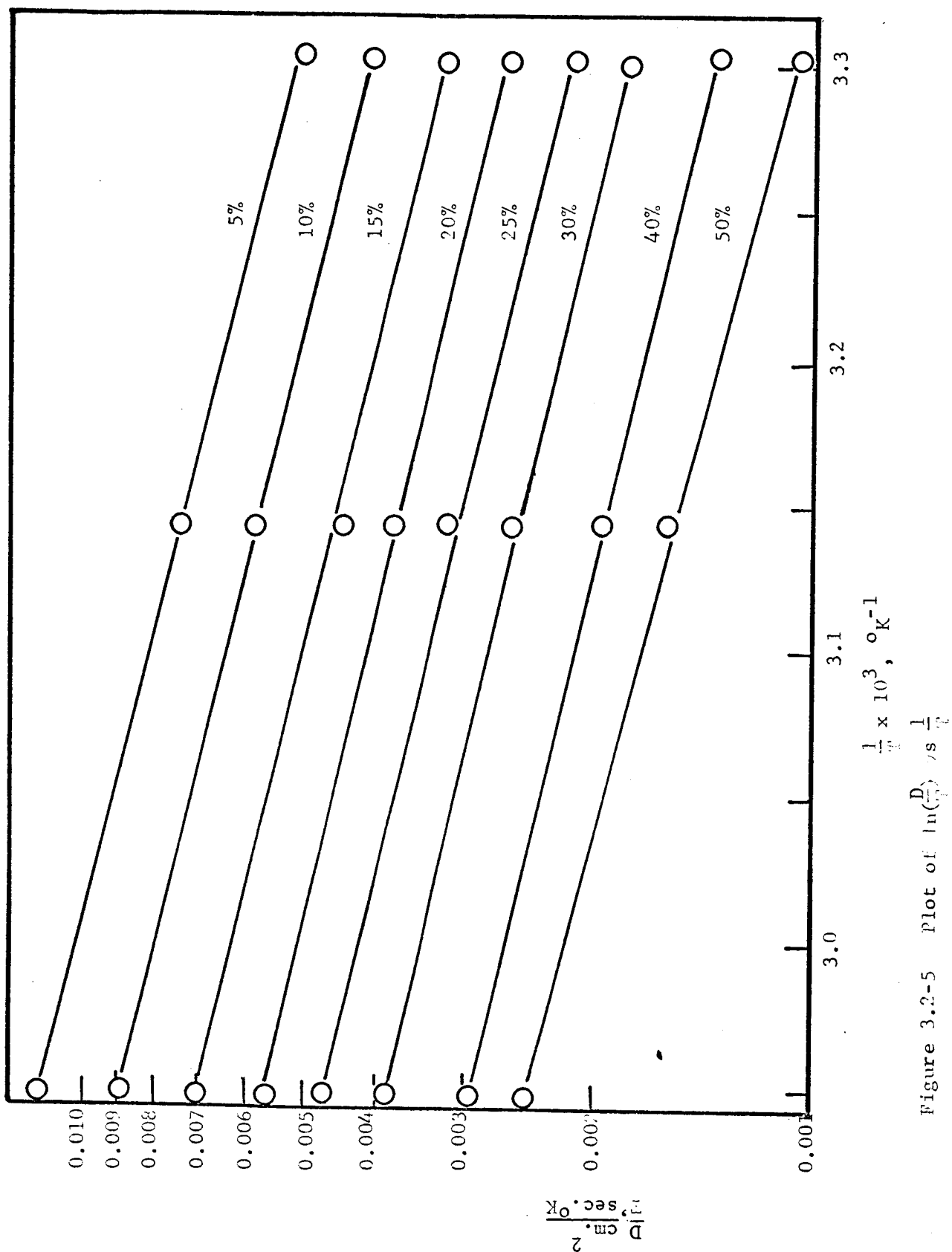


Figure 3.2-5 Plot of  $\ln\left(\frac{D}{T^2}\right)$  vs  $\frac{1}{T}$

#### 4.0 VAPOR PRESSURES OF LITHIUM HYDROXIDE SOLUTIONS - Jatinder Jolly

In order to measure or predict the solubility of oxygen and hydrogen in lithium hydroxide solutions it is necessary to know the exact vapor pressures of LiOH solutions at various LiOH concentrations and temperatures. As few such data are available in the literature, a suitable method was developed to measure the required data.

Several methods were studied and finally it was decided to adopt Cumming's (38) dew point method, suitably modified. It is believed that this method gives an accuracy of about  $0.01^{\circ}\text{C}$ , and the measurements can be extended to high vapor pressures. The method is also suitable for measurements over a large range of concentrations. It is a matter of indifference when using this method whether the system studied is liquid or solid.

##### 4.1 Apparatus

The apparatus consisted of a highly polished silver tube with closed end, which was silver-soldered to a stainless steel sleeve and closed at the top with a screwed cap. A thermometer ( $0.01^{\circ}\text{C}$  accuracy) and tubes, through which water was circulated to and from a constant temperature bath, were inserted through the cap. Two different outer enclosures were designed to suit different ranges of temperature and pressures. For vapor pressures up to 1 atmosphere the silver tube was fitted into a glass vessel containing the solution, as shown in Figure 4.1-1. One of the outlets of the glass container was connected by means of a vacuum glass stopcock to a vacuum pump to evacuate air from the system. The other outlet was connected to a manometer. Though the presence of air does not measurably affect the vapor pressure, the

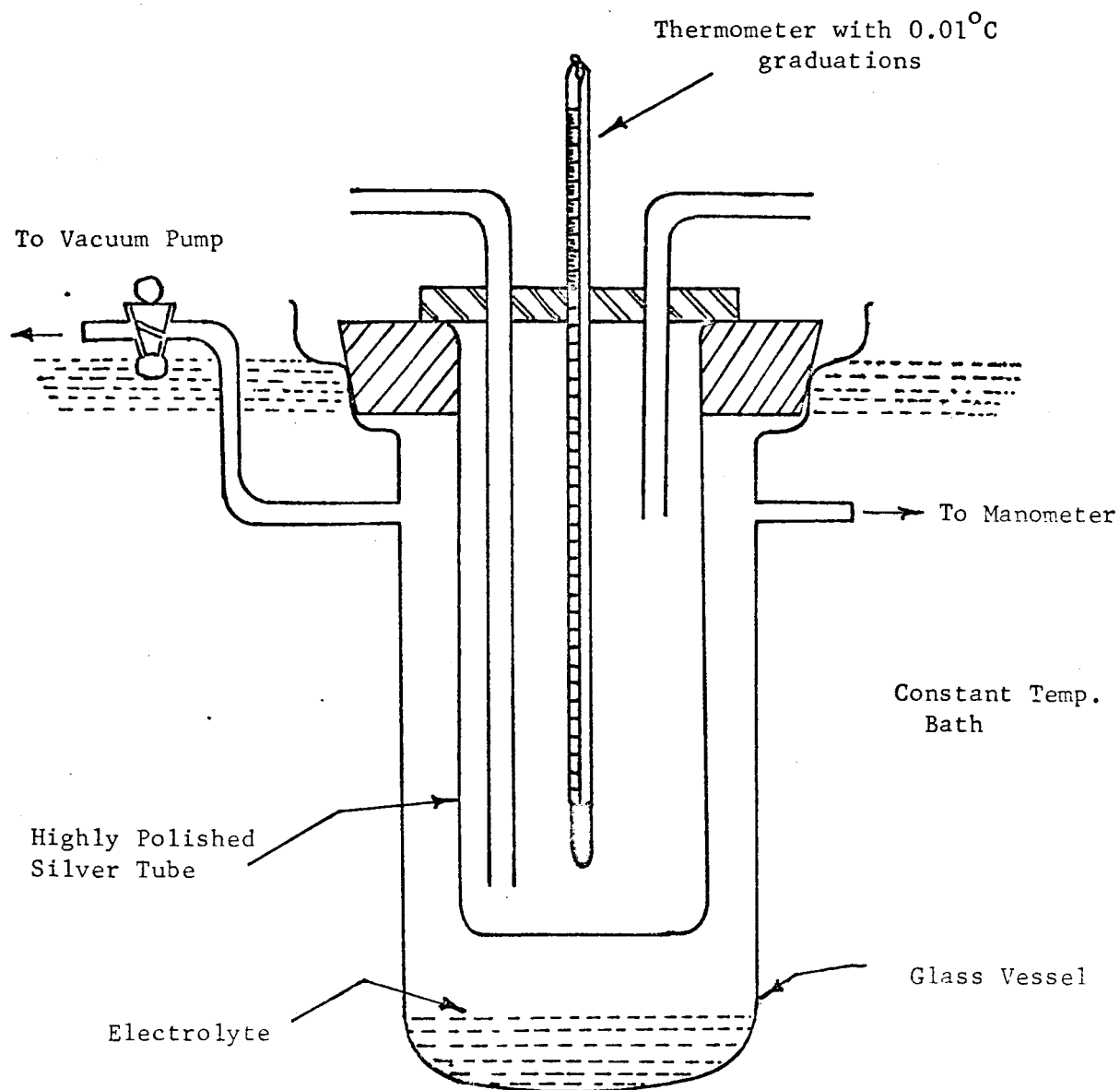


Figure 4.1-1 Glass Vapor Pressure Apparatus



formation and disappearance of dew is much sharper and more readily observed when air is absent. Sharpness of dewpoint is governed by the speed with which equilibrium is again set up after dew has been deposited or evaporated from the silver tube.

For higher temperatures and pressures, the silver tube was held as shown in Figure 4.1-2 in a stainless steel Tee, with the solution contained in a copper block extending from the bottom flange. The copper block was heavily silverplated, and it held about 40 ml of the solution. A side tube from the Tee could be connected with a vacuum pump.

#### 4.2 Experimental Procedure

Twenty ml. of solution was placed in the glass container (Figure 4.1-1), the silver tube affixed, and the apparatus evacuated. The vacuum pump was cut off and the evacuated apparatus was placed in a constant temperature bath, where it was allowed to remain until equilibrium was reached. A period of 30 minutes was found to be sufficient for this purpose. Hot water was circulated in and out of the silver tube from another constant temperature bath.

After equilibrating, the temperature of water being circulated in the silver tube was slowly reduced with the aid of the thermostat of the water circulating bath. The temperature was noted when the first traces of dew were formed on the silver tube. Thermometers used were high precision with  $0.05^{\circ}$  calibration up to  $40^{\circ}\text{C}$ ; for higher temperatures, the thermometer used had  $0.01^{\circ}\text{C}$  calibration. These thermometers were standardized against National Bureau of Standards corrected thermometers. Dew was made to disappear by slowly raising the temperature

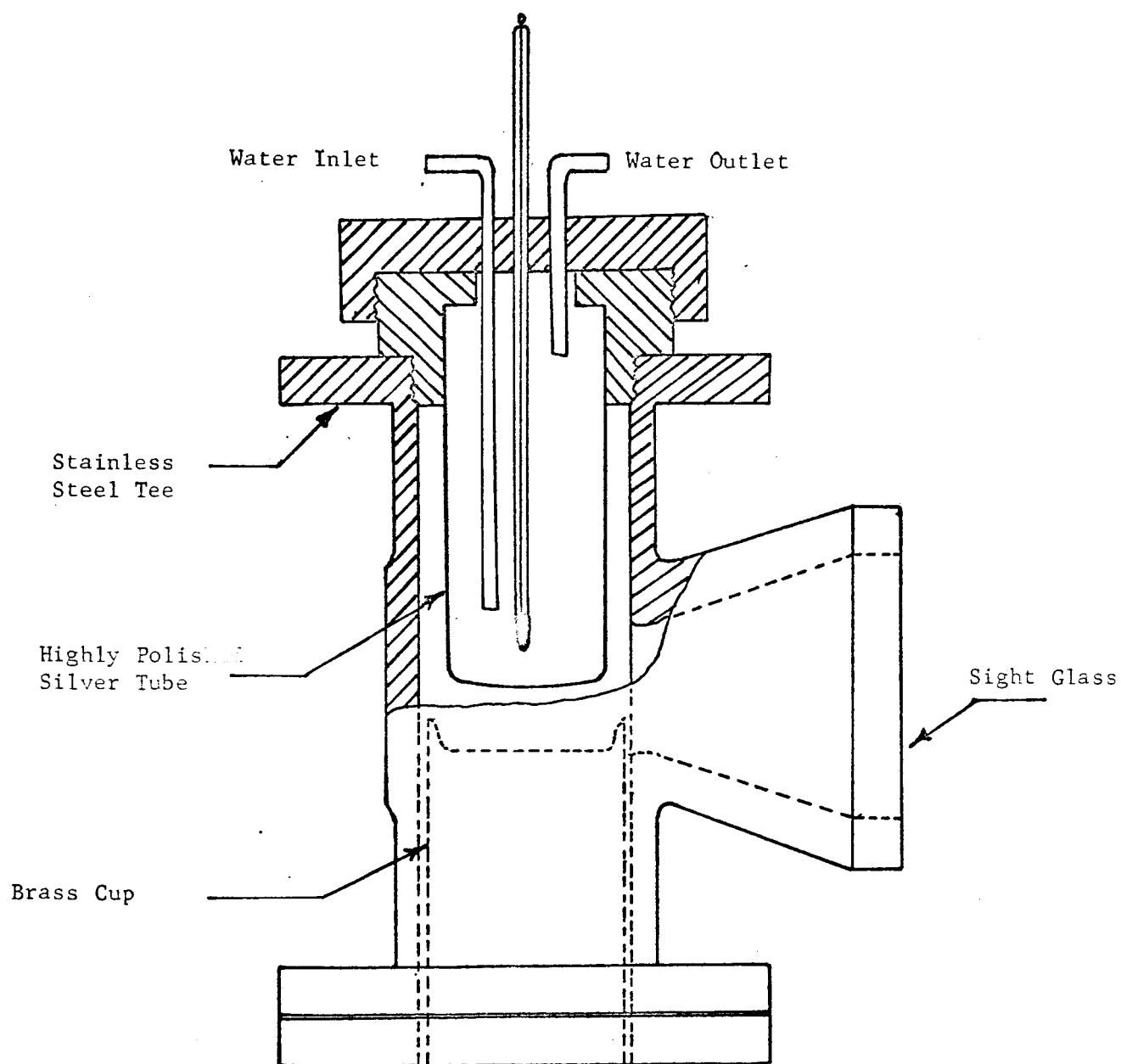


Figure 4.1-2. Stainless Steel Vapor Pressure Apparatus.

of the circulating water and the measurement then repeated. Using a highly polished tube, the point of appearance of dew with falling temperature was found to agree within  $0.05^{\circ}\text{C}$  with the point of disappearance of dew with rising temperatures. The values reported are the mean of these two values. In every determination the observation of dew-point was carried out at least three times, allowing a period of 15 minutes to elapse between each observation for equilibrium to be re-established. Determinations were not accepted unless the three results agreed within  $0.05^{\circ}\text{C}$ . The  $\text{LiOH}$  solution was standardized before and after the experiment with  $\text{HCl}$ . These dew-point temperatures were used to determine the vapor pressure from standard tables of vapor pressure of water in the literature. The vapor pressures over lithium hydroxide solutions are tabulated in Table 4.2-1 and are plotted on Figure 4.2-1.

#### 4.3 Experimental Results

The only literature data available for aqueous lithium hydroxide solutions (39) are for  $25^{\circ}\text{C}$ , and the results reported here agree very well, as may be seen in Table 4.2-1. The results at  $40^{\circ}$  and  $60^{\circ}$  are based on one experiment only; additional experiments will be performed to confirm the results at these temperatures. However, as extrapolated values at zero concentration compare favorably with the water vapor pressures at that temperature, these results appear to be satisfactory. Figure 4.3-1 shows a semilog plot of vapor pressure vs. reciprocal temperature. The linearity shown provides additional evidence concerning the accuracy of the data reported.

The work is being continued to get vapor pressures at higher temperatures.

TABLE 4.2-1  
VAPOR PRESSURES OF LITHIUM HYDROXIDE SOLUTIONS

<u>Temp. °C</u>	<u>Wt. % LiOH</u>	<u>Vapor Pressure Expt.</u>	<u>Vapor Pressure Lit. (39)</u>
25°C	0	23.75 mm Hg	23.756 mm Hg
	1.9	23.14	23.15
	3.85	22.56	22.55
	6.45	21.54	21.54
	8.05	21.12	21.10
	10.10	20.30	20.30
40°C	0	55.32	55.32
	1.9	53.88	
	3.85	52.16	
	8.05	49.02	
	10.10	46.58	
60°C	0	149.28	149.38
	2.4	144.11	
	4.82	139.79	
	8.52	132.82	
	10.2	129.13	

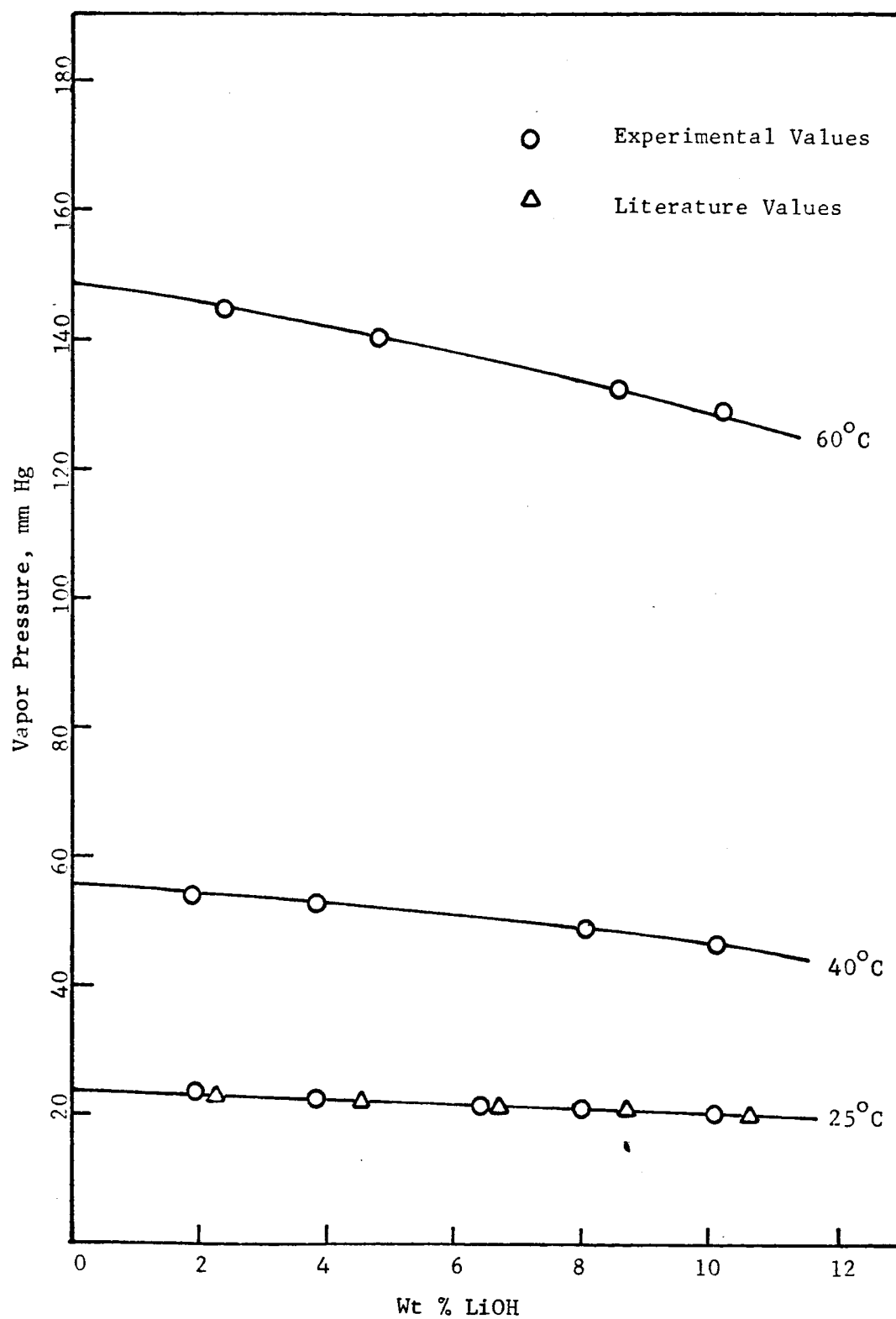


Figure 4.2-1 Vapor Pressure of LiOH vs Concentration

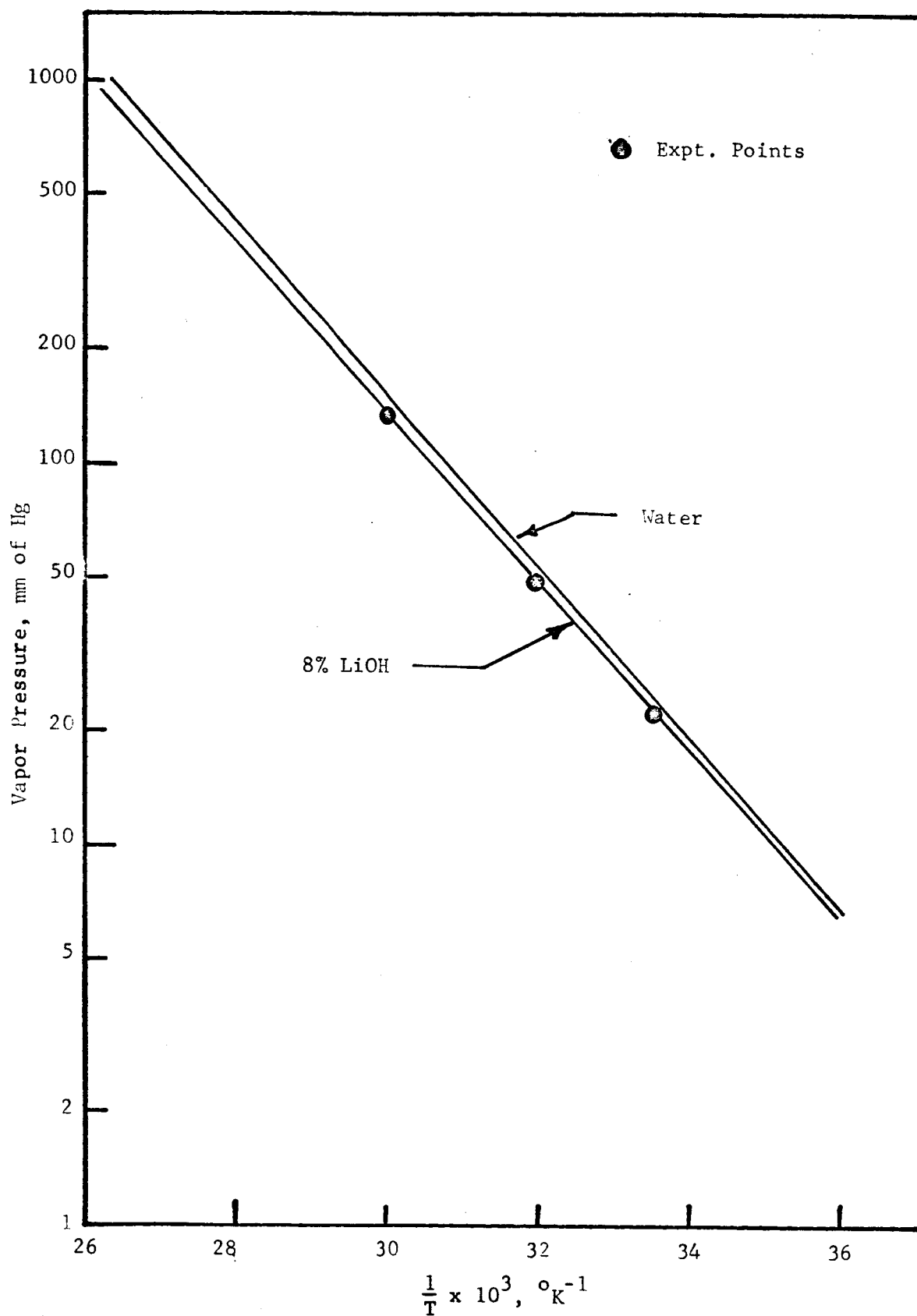


Figure 4.3-1. Vapor Pressure vs.  $\frac{1}{T}$  for LiOH Solutions.

## 5.0 SOLUBILITIES OF GASES IN LITHIUM HYDROXIDE SOLUTIONS - Jatinder Jolly

Solubilities of oxygen and argon in aqueous lithium hydroxide solutions have been measured at temperatures of 25, 40 and 60°C.

### 5.1 Experimental

The apparatus and experimental procedure used in these measurements was essentially the same as described in the Second Semi-Annual Report (40), with subsequent improvements given in the Third and Fourth Semi-Annual Reports (41,42).

### 5.2 Results

The experimental data for solubility of oxygen and argon have been tabulated in Table 5.2-1. As vapor pressure readings are needed to determine the solubility, these solubility measurements will be recalculated after doing more work on vapor pressures. In almost all cases the solubilities are the mean values for four or more replicate measurements. The absolute accuracy of the data is difficult to estimate as no data are available in the literature; however, a comparison of values of the solubility for pure water reported here with the literature values suggests that the accuracy is about  $\pm 2.0\%$ . The solubility values of oxygen and argon at 25, 40 and 60°C have been plotted against LiOH concentration in Figure 5.2-1.

Solubility of these gases decreased with temperature and LiOH concentration as shown in the graphs. The effect is less pronounced at higher concentrations than at lower ones.

Work on the solubility of other gases is being undertaken and will be presented in the next report.

TABLE 5.2-1  
SOLUBILITY OF GASES IN AQUEOUS LITHIUM HYDROXIDE SOLUTIONS

<u>Gas</u>	<u>Temperature</u>	<u>wt. °/LiOH</u>	<u>Solubility x 10<sup>3</sup> g. mole/liter</u>
Oxygen	25°C	0	1.263
		3.85	0.77
		5.85	0.587
		10.10	0.309
		Sat.	0.244
	40°C	0	1.045
		1.1	0.8715
		3.85	0.617
		8.05	0.3633
		10.1	0.265
		10.5	0.247
	60°C	0	0.875
		1.9	0.682
		3.85	0.502
		8.05	0.323
		10.1	0.243
Argon	25°C	0	1.36
		1.9	1.066
		3.85	0.8087
		8.05	0.4496
		10.1	0.329
	40°C	0	1.11
		1.9	0.896
		3.85	0.7055
		8.05	0.3877
		10.1	0.31
	60°C	0	0.918
		1.9	0.7655
		3.85	0.5816
		8.05	0.3609
		10.1	0.2849



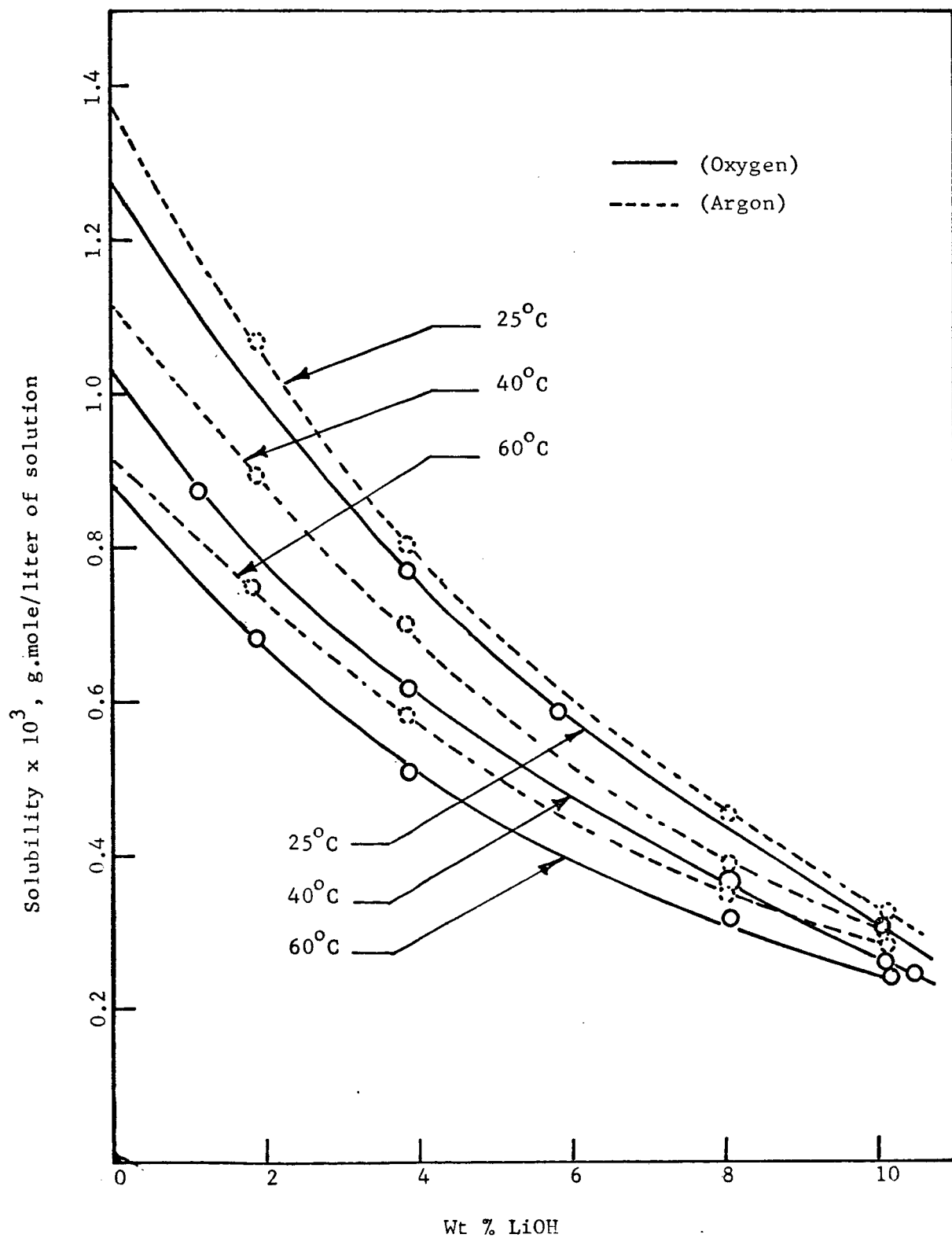


Figure 5.2-1 Solubility of Oxygen and Argon in LiOH Solutions

## 6.0 FUTURE PLANS

During the next period attention will be concentrated on completing diffusivity measurements for both hydrogen and oxygen in KOH solutions at temperatures up to about 100°C and concentration up to approximately saturation, and on the completion of solubility measurements in lithium hydroxide. In addition, it is planned to attempt to develop a more adequate theory for the diffusivity of the non-polar gases in concentrated solutions of electrolytes.

# REFERENCES CITED

1. Battino, R., and Clever, H. L., Chem. Rev., 66, 395 (1966).
2. Conway, B. E., Annual Rev. Phys. Chem., 17, 481 (1966).
3. Reiss, H., Friesch, H. L., Helfand, E., and Lebowitz, J. L., J. Chem. Phys., 32, 119 (1960).
4. Reiss, H., Friesch, H. L., Lebowitz, J. L., J. Chem. Phys., 31, 369 (1959).
5. Davidson, N., Statistical Mechanics, McGraw-Hill Book Co., Inc., New York (1962).
6. Pierotti, R. A., J. Phys. Chem., 67, 1840 (1963).
7. Pierotti, R. A., J. Phys. Chem., 69, 281 (1965).
8. Akerlof, G., Blender, P., J. Am. Chem. Soc., 63, 1085 (1941).
9. Tham, M. K., Gubbins, K. E., Walker, R. D., J. Chem. and Eng. Data, 12, 525 (1967).
10. Gubbins, K. E., Carden, S. N., and Walker, R. D., J. Gas Chromatog. 3, 98 (1965).
11. Geffcken, G., Zeit. Physik. Chemic, 49, 257 (1904)
12. Knaster, M. B., and Apel'baum, L. A., Russian J. Phys. Chem., 38, 120 (1964).
13. Ruetschi, P., and Amlie, R. F., J. Phys. Chem., 70, 718 (1966).
14. Davis, R. E., Horvath, Q. L., and Tobias, C. W., Electrochimica Acta, 12, 287 (1967).
15. Lange, N. A., (Ed.), Handbook of Chemistry, McGraw-Hill Book Co., New York (1961).
16. Morrison, T. J., and Johnstone, N. B., J. Chem. Soc., 76, 3441 (1954).
17. Lanning, A., J. Am. Chem. Soc., 76, 3294 (1954).
18. Friedman, H. L., J. Am. Chem. Soc., 76, 3294 (1954).
19. Bernal, J. D., and Fowler, R. H., J. Chem. Phys., 1, 515 (1933).
20. Landolt-Bornstein, Zahlenwerte Und Function Aus Physik-Chemie-Astronomic-Geophysik-Technik, Vol. I, Part 1 (1950).

21. Reed, T. M., J. Phys. Chem., 59, 428 (1955).
22. Bae, J. H., Ph.D. dissertation, University of Florida (1966).
23. Hirschfelder, J. O., Curtiss, C. F., Bird, R. B., Molecular Theory of Gases and Liquids, John Wiley and Sons, Inc., New York (1945).
24. Reed, T. M., Interactions Between Molecules, to be published.
25. Morgenau, Philosophy of Science, 8, 603 (1941).
26. Pauling, L., Proc. Roy. Soc., A114, 181 (1941).
27. Pauling, L., Wilson, E. B., Introduction to Quantum Mechanics, McGraw-Hill Book Company, Inc., New York (1935).
28. Debye, V. P., and McAulay, J. Physik, Z., 26, 22 (1925).
29. Ben-Naim, A., and Friedman, H. L., J. Phys. Chem., 71, 448 (1967).
30. Pierotti, R. A., J. Phys. Chem., 71, 2366 (1967).
31. Bockris, J. O'M., Bowler Reed, J., and Kitchener, J. A., Trans. Faraday Soc., 47, 184 (1951).
32. Damjanovic, A., Gemshaw, M. A., and Bockris, J. O'M., J. Electrochem. Soc. 114, 1107 (1967).
33. Makowski, M. P., Heitz, Ewald, and Yeagar, Ernest, J. Electrochem. Soc., 113, 204 (1966).
34. Davis, R. E., Horvath, G. L., and Tobias, C. W., Electrochimica. Acta, 12, 287 (1967).
35. Ruetschi, P., J. Electrochem. Soc. 114, 303 (1967).
36. Ratcliff, G. A., and Holdcroft, J. G., Trans. Instn. Chem. Engrs., 41, 315 (1963).
37. Bhatia, K. K., M.S. Thesis, University of Florida (1965).
38. Cumming, A. C., J. Chem. Soc., 95, 1772 (1909).
39. Walter, K. and Groeneveld, A., Zietschrift fur Physikahsche, Chemie Neve Folge, 32, S(110-126) (1962).
40. Walker, R. D., Second Semi-Annual Report, March, 1966, NASA Research Grant NGR 10-005-022.

41. Walker, R. D., Third Semi-Annual Report, September, 1966, NASA Research Grant NGR 10-005-022.
42. Walker, R. D., Fourth Semi-Annual Report, March, 1967, NASA Research Grant NGR 10-005-022.